

KGE Calibrator: An Efficient Probability Calibration Method of Knowledge Graph Embedding Models for Trustworthy Link Prediction

Anonymous ACL submission

Abstract

Knowledge graph embedding (KGE) models are designed for the task of link prediction, which aims to infer missing triples by learning accurate representations for entities and relations within a knowledge graph. However, existing KGE research largely overlooks the issue of probability calibration, leading to uncalibrated probability estimates that fail to reflect the true correctness of predicted triples, potentially resulting in erroneous decisions. Moreover, current calibration methods are not well-suited for KGE models, and no dedicated probability calibration method has been specifically designed for them. In this paper, we propose KGE Calibrator (KGEC), the first probability calibration method tailored for KGE models to enhance the trustworthiness of their predictions. To achieve this, we introduce a Jump Selection Strategy that improves efficiency by selecting the most informative instances while filtering out less significant ones. We also propose Multi-Binning Scaling, which models different probability levels separately to increase the model’s capacity and flexibility. Additionally, we propose a Wasserstein distance-based loss function to further boost calibration performance. Extensive experiments across multiple datasets demonstrate that KGEC consistently outperforms existing calibration methods in terms of both effectiveness and efficiency, making it a promising solution for probability calibration in KGE models.

1 Introduction

Knowledge graphs (KGs) are essential resources for a wide range of knowledge-driven tasks, including semantic search (Xiong et al., 2017), knowledge reasoning (Liu et al., 2021), question answering (Shen et al., 2019; Ye et al., 2023), and reading comprehension (Yang et al., 2019; Meng et al., 2023). Prominent large-scale KGs such as YAGO (Suchanek et al., 2007), DBpedia (Lehmann et al.,

| Query: (Greece, _member_of_domain_region, ?) | |
|--|---------------------|
| True answer: sibyl | |
| Ranked candidate entities | Uncalibrated scores |
| Greece | -0.1873 |
| Holy_See | -0.2946 |
| sibyl | -0.5992 |
| Colosseum | -0.8017 |
| Sistine_Chapel | -0.8683 |

Figure 1: A real example from the WN18RR (Dettmers et al., 2018) dataset, where ranked candidate entities and their corresponding uncalibrated scores are produced by TransE (Bordes et al., 2013) model. In this example, the correct tail entity “sibyl” is ranked third, demonstrating that existing KGE models perform well under ranking metrics. However, all predicted scores are negative, indicating a lack of trustworthy probability estimates and highlighting the need for probability calibration in KGE models.

2015), and Freebase (Bollacker et al., 2008) encompass millions of entities and hundreds of millions of relational facts, which are typically structured as sets of $\langle head\ entity, relation, tail\ entity \rangle$ triples.

However, most KGs are incomplete due to extraction errors and limited input resources. This makes link prediction, also known as knowledge graph completion, crucial for inferring missing links and improving KG quality. To this end, knowledge graph embedding (KGE) models such as TransE (Bordes et al., 2013) and ComplEx (Trouillon et al., 2016) tackle this problem by learning latent representations of entities and relations to score the plausibility of candidate triples. Beyond link prediction, KGE models have demonstrated remarkable success across diverse applications, including entity alignment (Sun et al., 2018) and canonicalization (Shen et al., 2022).

While the accuracy of KGE models has seen significant advancements, the critical issue of probability calibration remains largely overlooked. Specifi-

cally, KGE models should output calibrated probabilities alongside their predictions. However, they typically produce uncalibrated scores (Pezeshkpour et al., 2020; Tabacof and Costabello, 2020). This stems from link prediction being framed as a ranking task, where metrics like HITS@N and Mean Rank (MR) prioritize relative ordering while ignoring the reliability of output scores. As a result, models can assign implausible scores to correct entities yet still perform well, as shown in Figure 1. Such limitations hinder their use in high-stakes domains such as drug and protein target discovery (Zeng et al., 2022; Mohamed et al., 2020), where trustworthy probabilities are essential.

To address this critical issue, increasing attention has been directed toward the probability calibration task of KGE models, which aims to convert the uncalibrated scores assigned to candidate triples into well-calibrated probability estimates. As a post-processing technique, calibration improves the trustworthiness of link prediction results, making them more reliable for downstream applications. However, probability calibration in KGE poses unique challenges compared to traditional classification. Image classification datasets like CIFAR-100 (Krizhevsky et al., 2009) or document classification datasets like SST (Socher et al., 2013) involve tens or hundreds of classes. In contrast, KGE tasks treat each entity as a distinct class, leading to massive class spaces (e.g., FB15K and WN18 have 14,951 and 40,943 entities, respectively). This high cardinality leads to tiny per-class probabilities and makes the calibration process extremely sensitive. Even minor perturbations can distort the original ranking and negatively impact link prediction performance. Therefore, preserving the original ranking quality becomes a critical requirement, posing a distinctive challenge for probability calibration in the KGE setting.

Despite its importance and unique challenges, probability calibration in KGE remains largely underexplored. Prior studies (Tabacof and Costabello, 2020; Pezeshkpour et al., 2020) have shown that popular KGE models produce poorly calibrated scores, resulting in unreliable probability estimates. Several off-the-shelf calibration methods, such as Platt Scaling, Isotonic Regression, and Temperature Scaling, have been evaluated (Safavi et al., 2020; Zhu et al., 2022), but these methods are designed for standard classifiers and are not well-suited to the scale and ranking-sensitive nature of KGE. A few works have explored calibration in spe-

cific tasks, including triple classification (Tabacof and Costabello, 2020), relation prediction (Safavi et al., 2020), and low-dimensional entity embedding transformations (Wang et al., 2021). However, no existing approach offers a calibration method explicitly tailored to the probabilistic characteristics of KGE models. This leaves a critical gap in improving the trustworthiness of KGE-based link prediction.

To fill this gap, we propose KGE Calibrator (KGEC), the first probability calibration method tailored specifically for KGE models. To enhance training efficiency under the large-scale class space characteristic of KGE, we introduce the Jump Selection Strategy, which selects the most informative instances while discarding less significant ones. To increase model expressiveness and better captures the ranking-sensitive nature of KGE predictions, we propose Multi-Binning Scaling, which models different probability levels separately, thereby increasing model capacity and flexibility. Additionally, we propose a Wasserstein distance-based loss function to further boost calibration performance. To the best of our knowledge, this is the first use of the Wasserstein distance for probability calibration.

Contributions. Our major contributions can be summarized as follows:

- We evaluate nine widely used post-processing calibration methods and find that four of them are unsuitable for entity prediction due to their poor performance, which alters the original link prediction results after calibration.
- We propose KGEC, the first probability calibration method specifically designed for KGE models, which addresses the challenge of large class space in calibration while preserving the original ranking performance.
- A thorough experimental study over four datasets demonstrates that KGEC consistently outperforms existing calibration methods in both performance and efficiency.

2 Related Work

Probability Calibration in KGE Models. Several studies have highlighted the lack of well-calibrated probability estimates in KGE models. Early work by (Tabacof and Costabello, 2020) and (Pezeshkpour et al., 2020) showed that widely used KGE models are poorly calibrated in triple classification tasks. To address this, (Tabacof and Costabello, 2020) applied Platt Scaling (Platt et al., 1999) and Isotonic Regression (Zadrozny

and Elkan, 2002), while (Safavi et al., 2020) explored Matrix Scaling and Vector Scaling (Guo et al., 2017) in relation prediction. A broader evaluation by (Zhu et al., 2022) tested additional off-the-shelf calibration techniques, including Histogram Binning (Zadrozny and Elkan, 2001), Beta Calibration (Kull et al., 2017), and Temperature Scaling (Guo et al., 2017) for triple classification. Furthermore, (Rao, 2021) examined calibration under both closed-world and open-world assumptions. While these works shed light on the calibration issue in KGE, they all rely on existing techniques originally designed for traditional classification problems. None propose a calibration method specifically tailored for KGE models, leaving a critical gap in the literature.

Expit Transformations. Expit transformations aim to convert uncalibrated scores into probabilities using functions such as the Sigmoid (Nickel et al., 2015; Tabacof and Costabello, 2020; Zhu et al., 2022) and Softmax (Pezeshkpour et al., 2020). More approaches include neighborhood intervention consistency (NIC) (Wang et al., 2021) and min-max scaling (Rao, 2021). However, recent research has shown that even when expit-transformed scores can be interpreted as probabilities, they are still uncalibrated and unreliable (Zhu et al., 2022). As a result, these expit transformations are generally viewed as a preliminary step, typically followed by a dedicated calibration method such as Platt Scaling or Isotonic Regression. In fact, (Zhu et al., 2022) concluded that expit transformations are ineffective in most cases and suggested probability calibration as a better approach. Following this direction, our work focuses exclusively on probability calibration and does not include expit transformations as part of our method design.

3 Preliminaries

3.1 Knowledge Graph

A knowledge graph (KG) $\mathcal{G} = \{\xi\}$ contains a set of triples $\xi = (h, r, t)$, where each triple includes a head entity $h \in \mathcal{E}$, a tail entity $t \in \mathcal{E}$, and a relation $r \in \mathcal{R}$ connecting head and tail. \mathcal{E} and \mathcal{R} refer to the set of all entities and relations of \mathcal{G} respectively. $N = |\mathcal{E}|$ and $M = |\mathcal{R}|$ denote the number of entities and relations respectively.

3.2 Knowledge Graph Embeddings

Knowledge graph embedding (KGE) models aim to represent each head entity h , relation r , and tail

entity t from a KG \mathcal{G} as d -dimension continuous embeddings \mathbf{h} , \mathbf{r} , and $\mathbf{t} \in \mathbb{R}^d$. Each KGE model defines a model-specific score function ψ that assigns a score to each triple $\xi = (h, r, t)$ based on its corresponding embeddings, i.e., $\psi(\xi) = \psi(\mathbf{h}, \mathbf{r}, \mathbf{t})$. Table 3 in Appendix A lists the score functions of the most popular KGE models.

3.3 Link Prediction

Link prediction, the primary task for KGE models, includes entity and relation prediction. Entity prediction is more challenging due to the large number of candidate entities. For example, WN18RR (Dettmers et al., 2018) contains 40,943 entities but only 11 relations. This paper focuses on the more difficult entity prediction task. To be specific, the entity prediction includes head and tail prediction. For head prediction, given a query of the form $(?, r, t)$, each entity $e_i \in \mathcal{E}$ becomes a potential candidate for the head entity. The trained KGE model assigns a score $\psi(\xi_i)$ to each triple $\xi_i = (e_i, r, t)$, where e_i is a candidate head entity, and r and t are the given relation and tail entity. These scores are then ranked, with higher-ranked triples being more plausible, indicating that the corresponding entity e_i is a likely answer to the query $(?, r, t)$. The task of tail entity prediction could be defined in a similar manner.

4 KGE Calibrator

In this section, we present our proposed method, KGE Calibrator (KGEC). We begin with the introduction of our proposed Jump Selection Strategy and Multi-Binning Scaling, thereafter describe the Wasserstein distance-based loss function subsequently.

4.1 Jump Selection Strategy

To improve training efficiency in the context of large-scale class spaces inherent to KGE tasks, it is crucial to focus on the most informative instances while discarding less significant one during training the calibration method. Inspired by (Shen et al., 2022), we propose the Jump Selection Strategy, which selects the most significant instances for training rather than using all available instances. This Jump Selection Strategy is summarized in Algorithm 1, and we elaborate it as follows.

Given a query set $Q = \{q_1, \dots, q_i, \dots, q_N\}$ where $q_i = (?, r_i, t_i)$, and a set of candidate entities $\mathcal{E} = \{e_1, \dots, e_i, \dots, e_M\}$, we first generate candidate triples $\xi_{ij} = (e_j, r_i, t_i)$ for all i and j (line 1

Algorithm 1 Jump Selection Strategy

Input: A set of queries $Q = \{q_1, \dots, q_i, \dots, q_N\}$, where $q_i = (?, r_i, t_i)$ for $i = 1, \dots, N$, a set candidate entities $\mathcal{E} = \{e_1, \dots, e_j, \dots, e_M\}$ for $j = 1, \dots, M$, a trained KGE model ψ

- 1: **Generate** candidate triples for each query: $\xi_{ij} \leftarrow (e_j, r_i, t_i)$
- 2: **Compute** uncalibrated scores for each query: $x_{ij} \leftarrow \psi(\xi_{ij}) = \psi(\mathbf{e}_j, \mathbf{r}_i, \mathbf{t}_i)$
- 3: Form the uncalibrated scores into a score vector: $\mathbf{X}_i \leftarrow \{x_{i1}, \dots, x_{ij}, \dots, x_{iM}\}$
- 4: **Compute** probabilities: $\mathbf{P}_i \leftarrow \sigma_{SM}(\mathbf{X}_i)$ for each query
- 5: Form the uncalibrated probabilities into a probability matrix: $\mathbf{P} \leftarrow \{\mathbf{P}_1, \dots, \mathbf{P}_i, \dots, \mathbf{P}_N\}^\top$
- 6: **Sort** \mathbf{P} in descending order by row to obtain $\tilde{\mathbf{P}}$
- 7: **for** $j = 1$ **to** $M - 1$ **do**
- 8: $J_j \leftarrow D_{KL}(\tilde{\mathbf{P}}_j \parallel \tilde{\mathbf{P}}_{j+1})$
- 9: **end for**
- 10: $J^* \leftarrow \arg \max_j J_j$
- 11: $p^* \leftarrow \tilde{\mathbf{P}}_{J^*}$

Output: Selected index J^* and its corresponding probability p^* for calibration

in Algorithm 1). The KGE model ψ is then used to compute uncalibrated scores $x_{ij} = \psi(\xi_{ij})$ for each candidate triple, forming a score vector \mathbf{X}_i for each query q_i (lines 2 – 3 in Algorithm 1). These scores are transformed into probability vectors \mathbf{P}_i via the Softmax function σ_{SM} , and assembled into a probability matrix \mathbf{P} (lines 4 – 5 in Algorithm 1). We then sort each row of \mathbf{P} in descending order to obtain $\tilde{\mathbf{P}}$ (line 6 in Algorithm 1), so that higher probabilities appear first. To identify the most informative instance, we compute the Jump Measure J_j for each adjacent column pair in the sorted probability matrix $\tilde{\mathbf{P}}$ using KL divergence (lines 7 – 8 in Algorithm 1). The index J^* corresponding to the maximum Jump Measure is then selected, and its associated probability vector $p^* = \tilde{\mathbf{P}}_{J^*}$ is used as the most informative sample for subsequent calibration training (lines 9 – 11 in Algorithm 1).

4.2 Multi-Binning Scaling

Temperature Scaling (TS) (Guo et al., 2017) is a widely used post-hoc calibration method due to its simplicity and its ability to preserve the original model’s ranking order, which is an essential property in the KGE link prediction task. TS achieves

this by scaling the uncalibrated probabilities using a single scalar temperature parameter $T > 0$, thereby maintaining the relative ordering of scores. However, TS suffers from limited expressiveness, as it applies the same transformation regardless of the input probability magnitude (e.g., both 0.1 and 0.9 are scaled identically), which can lead to suboptimal calibration performance.

To address this limitation, we introduce Multi-Binning Scaling (MBS), a more flexible approach that maintains the ranking-preserving property of TS while improving calibration quality. Inspired by histogram binning (Zadrozny and Elkan, 2001), we partition the uncalibrated probabilities $p^* = \{p_1^*, \dots, p_i^*, \dots, p_N^*\}$ into W mutually exclusive bins $B_1, \dots, B_w, \dots, B_W$. Each bin is associated with an independent scalar temperature parameter T_w . Uncalibrated probabilities falling into bin B_w are calibrated using:

$$\hat{p}_i = \sigma_{SM}(p_i^*/T_w^2), \quad (1)$$

where σ_{SM} denotes the Softmax function. The squared temperature form follows convention in temperature-based calibration and provides smoother gradient behavior.

To define bin boundaries, we divide the interval $[0, 1]$ into W equal-length segments:

$$0 = a_1 \leq a_2 \leq \dots \leq a_{W+1} = 1, \quad (2)$$

so that bin B_w corresponds to the interval $(a_w, a_{w+1}]$. In this paper, we adopt uniformly divided equal-length intervals for bin boundaries to maintain simplicity. More advanced strategies, such as adaptive bin boundaries, are left for future exploration.

For probability vectors $p^- = \tilde{\mathbf{P}}_j$ where $j \neq J^*$ (i.e., those not selected by Jump Selection Strategy), we reuse the temperature parameter T_m associated with p^* to calibrate them. This design avoids the overhead of rebinning and retraining temperature parameters, while ensuring that the original ranking produced by the model remains unaffected. Overall, MBS combines the ranking-preserving property of TS with the expressiveness of bin-based transformations, enabling more accurate and robust calibration for KGE link prediction without compromising original ranking performance.

4.3 Optimization

While Kullback–Leibler (KL) divergence is a commonly used loss function in deep learning, it poses

notable limitations for probability calibration in KGE models. This is particularly evident in high-cardinality tasks such as entity prediction, where each entity corresponds to a unique class and the class space can include tens of thousands of candidate entities. First, in such large class spaces, the predicted probabilities for most entities are extremely small. When the true label probability q_i is nonzero but the predicted probability p_i approaches zero, the corresponding KL loss becomes negligible. This results in near-zero loss values for many informative instances, reducing their impact during training and weakening the effectiveness of calibration. Second, KL divergence towards infinity when $p_i > 0$ and q_i approaches zero, causing the loss to diverge toward infinity. In practice, this can cause gradient instability or explosion, particularly in sparse or imbalanced prediction scenarios. These issues compromise the robustness and reliability of probability calibration in KGE. A detailed analysis is provided in Appendix B.

To address these issues, we propose using the Wasserstein distance as the loss function for KGEC. Unlike KL divergence, the Wasserstein distance provides a more stable and geometrically meaningful way to compare probability distributions by considering the minimum cost of transforming one distribution into another. This perspective is especially valuable in calibration, where we aim to align uncalibrated scores with true probability distributions while preserving their structure.

The Wasserstein distance models calibration as an optimal transport (OT) problem, where the goal is to find the most efficient way to move probability mass from the uncalibrated distribution p^* to the target distribution q . The feasible set of transport plans is defined by the transportation polytope $U(p^*, q)$, which contains all nonnegative transport matrices P :

$$U(p^*, q) = \{P \in \mathbb{R}_+^{d \times d} | P\mathbf{1}_d = p^*, P^\top \mathbf{1}_d = q\}, \quad (3)$$

where $\mathbf{1}_d \in \mathbb{R}^d$ is a vector of ones.

Given a cost matrix $M \in \mathbb{R}^{d \times d}$, the Wasserstein distance is defined as the minimum transport cost required to map p^* to q using the transport matrix P .

$$D_{WD}(p^*, q) = \min_{P \in U(p^*, q)} \langle P, M \rangle = \sum_{m,n} P_{m,n} M_{m,n}, \quad (4)$$

where $\langle \cdot, \cdot \rangle$ stands for the Frobenius dot-product and $M_{m,n} = |p_m^* - q_n|$ represents the absolute

difference between the m -th and n -th elements of p^* and q .

To improve computational efficiency, we use the Sinkhorn distance (Cuturi, 2013), which provides a fast approximation to the constrained Wasserstein distance by introducing entropy regularization. Given the OT plan P^λ and cost matrix M , the Sinkhorn distance is defined as follows:

$$D_{SD}(p^*, q) = \langle P^\lambda, M \rangle, \quad (5)$$

where $\lambda > 0$ is the weight for entropy regularization. The OT plan P^λ is obtained by solving:

$$P^\lambda = \arg \min_{P \in U(p^*, q)} \langle P, M \rangle - \frac{1}{\lambda} h(P), \quad (6)$$

where $h(P)$ is the entropy of P . The solution P^λ computed iteratively via Sinkhorn normalization (Cuturi, 2013) as follows:

$$\begin{aligned} u^t &= p^* \oslash (K^\top v^{t-1}), \\ v^t &= q \oslash (K u^t), \end{aligned} \quad (7)$$

where \oslash indicates element-wise division, t denotes the iteration time, and $K = \exp(-\frac{M}{\lambda})$ is the kernel matrix with entropy regularization weight λ . Finally, the optimal transport plan P^λ is given by:

$$P^\lambda = \text{diag}(v^t) K \text{diag}(u^t), \quad (8)$$

This Sinkhorn-regularized Wasserstein loss enables more stable optimization and improves calibration performance, particularly under the large class space settings encountered in KGE tasks.

5 Experiments

For the experiments, we first introduce three key research questions (RQs), and then use our experimental results to address each of these questions individually.

- **RQ1:** Which of the existing post-processing calibration methods can not affect the KGE results?

- **RQ2:** Can our proposed KGEC method surpass the performance of existing methods while preserving the original ranking quality?

- **RQ3:** Is our proposed KGEC method efficient?

Section 5.1 details the datasets used in our experiments, along with the training and learning processes for both the link prediction models and calibration functions. Section 5.2 presents the ranking results evaluation for **RQ1**. Section 5.3 presents the effectiveness evaluation for **RQ2**. Section 5.4 discusses the training time and memory usage for **RQ3**.

5.1 Experimental Setting

5.1.1 datasets

We evaluate our proposed model on four popular datasets, which are commonly used to evaluate link prediction, where FB15K (Bordes et al., 2013) and FB15K-237 (Toutanova and Chen, 2015) were extracted from Freebase (Bollacker et al., 2008), WN18 (Bordes et al., 2013) and WN18RR (Dettmers et al., 2018) were extracted from WordNet (Miller, 1995). Note that FB15K-237 and WN18RR are subsets of FB15K and WN18, respectively, in which near-same and near-reverse relations have been removed. These datasets are publicly available, and already partitioned into training, validation and testing splits. The statistics of them are summarized into Table 4 in Appendix C.

5.1.2 KGE models

To evaluate our proposed model, we leverage four famous KGE models in our experiments, i.e., TransE (Bordes et al., 2013), DistMult (Yang et al., 2015), ComplEx (Trouillon et al., 2016), and RotatE (Sun et al., 2019). The score functions of them are shown in Table 3. It is noted that any KGE models could be employed as the input of our KGEC model, as long as it could encode triples into embeddings and get their scores. Therefore, choosing different KGE models is not the focus of this paper and left for future exploration.

5.1.3 Calibration baselines

All calibration baselines are listed as follows.

- Platt Scaling (PS) (Platt et al., 1999) is a parametric approach to calibration, which is based on transforming the non-probabilistic outputs of a binary classifier to calibrated confidence scores.
- Histogram Binning (HB) (Zadrozny and Elkan, 2001) is a simple non-parametric calibration method. All uncalibrated predictions are divided into mutually exclusive bins, where each bin is assigned a calibration score.
- Isotonic Regression (IR) (Zadrozny and Elkan, 2002) is a strict generalization of histogram binning in which the bin boundaries and bin predictions are jointly optimized.
- Bayesian Binning into Quantiles (BBQ) (Naeini et al., 2015) is an extension of histogram binning using the concept of Bayesian model averaging.
- Matrix Scaling (MS) and Vector Scaling (VS) (Guo et al., 2017) are two multi-class extensions of Platt scaling.

• Temperature Scaling (TS) (Guo et al., 2017) is the simplest extension of Platt scaling, uses a single scalar parameter $T > 0$ for all candidates.

• Meta-Cal (Ma and Blaschko, 2021) integrates bipartite-ranking model with selective classification to improve calibration map.

• Parametrized Temperature Scaling (PTS) (Tomani et al., 2022) is the generalization of temperature scaling by computing prediction-specific temperatures, parameterized by a neural network.

In this work, we focus exclusively on post-hoc probability calibration methods to preserve the original ranking of KGE models. As such, techniques that modify model training, such as regularization (Ahn et al., 2019), ensemble (Lakshminarayanan et al., 2017), MC-dropout (Gal and Ghahramani, 2016) and mixup (Thulasidasan et al., 2019), are beyond the scope of this study. Additionally, we fail to report results for Beta Calibration (Kull et al., 2017) due to its extremely high computational cost. For instance, even on the smallest dataset (WN18RR), this method required over 60 hours to complete, rendering it impractical for our large-scale experiments. Lastly, we clarify that this work focuses solely on probability calibration and does not consider exit transformations, such as replacing the Softmax function with Sigmoid or NIC (Wang et al., 2021). These transformations are thus fall outside the scope of our study.

5.1.4 Evaluation measures

Evaluating calibration performance requires both reliable metrics to detect miscalibration and effective techniques to fix such distortion. In this work, we adopt three widely used evaluation metrics: Expected Calibration Error (ECE) (Naeini et al., 2015), Adaptive Calibration Error (ACE) (Nixon et al., 2019), and Negative Log-Likelihood (NLL). Each metric captures different aspects of calibration quality. Due to space constraints, we refer readers to (Naeini et al., 2015; Nixon et al., 2019) for detailed formulations. To give an overall evaluation of each method, we calculate the average of each metric for different dataset and different KGE models as **Average**, which is a standard comprehensive metric for the task of KGE calibration.

5.1.5 Setting details

To ensure a fair comparison, all baselines and metrics we used are from third-party frameworks or their original codes. Specifically, the code of PS,

HB, IR, BBQ, and TS are from net:cal¹. The code of MS and VS and all metrics are calculated by the TorchUncertainty². The code of Meta-Cal³ and PTS⁴ is from their official code. For the hyper-parameter setting of KGEC, the number of bins is set to 10, the learning rate is set to 0.01, the batch size is set to 32, the initial temperature for each bin is set to 1.0 and the optimizer is AdamW (Loshchilov and Hutter, 2019). Except for VS, MS, and TS which uses the *Multiclass* setting, all other baselines use the *One-vs-all* setting to avoid unacceptable training time. We follow the closed world assumption in our experiments. This is because the open world assumption requires a label for each triplet, which is missing in existing datasets. All experimental results are the average values obtained after running 10 times. We make the source code used in this paper publicly available for future research⁵.

5.2 Accuracy Affection Study for RQ1

Table 1 presents the results of the TransE model across various datasets after applying different calibration methods. The Uncal row represents the original, uncalibrated results, \uparrow indicates an improvement, while \downarrow indicates a decline compared to the original uncalibrated results. Among the reported evaluation metrics: A lower Mean Rank (MR) indicates better performance. Higher values of Mean Reciprocal Rank (MRR), HITS@1, HITS@3, and HITS@10 indicate better performance. For more results of other KGE models across various datasets after applying different calibration methods are shown in Table 8, Table 9 and Table 10.

From the experimental results in Table 1, we can see that (1) HB, IR, BBQ, MS, and Meta-Cal significantly degrade performance across all four datasets, making them unsuitable as calibrators for KGE models in the entity prediction task; (2) KGEC maintains the ranking accuracy across all datasets, demonstrating their effectiveness as the most suitable calibration methods for this task; (3) PS, VS, and TS either preserve or slightly improve accuracy on WN18 and WN18RR and generally do not lead to performance deterioration; (4) VS

Table 1: Effect of different calibration methods on the performance of the TransE model across various datasets.

| Method | MR | MRR | HITS@1 | HITS@3 | HITS@10 |
|------------------|--------------------|--------------------|--------------------|--------------------|--------------------|
| WN18 | | | | | |
| Uncal | 263 | 0.772 | 0.706 | 0.807 | 0.920 |
| PS | 260 \uparrow | 0.772 | 0.706 | 0.807 | 0.920 |
| HB | 15299 \downarrow | 0.225 \downarrow | 0.212 \downarrow | 0.236 \downarrow | 0.240 \downarrow |
| IR | 14590 \downarrow | 0.251 \downarrow | 0.232 \downarrow | 0.267 \downarrow | 0.279 \downarrow |
| BBQ | 15178 \downarrow | 0.218 \downarrow | 0.200 \downarrow | 0.233 \downarrow | 0.244 \downarrow |
| VS | 258 \uparrow | 0.772 | 0.706 | 0.807 | 0.920 |
| MS | 16483 \downarrow | 0.013 \downarrow | 0.005 \downarrow | 0.013 \downarrow | 0.029 \downarrow |
| TS | 260 \uparrow | 0.772 | 0.706 | 0.807 | 0.920 |
| Meta-Cal | 1784 \downarrow | 0.718 \downarrow | 0.657 \downarrow | 0.749 \downarrow | 0.856 \downarrow |
| PTS | 2116 \downarrow | 0.751 \downarrow | 0.706 | 0.775 \downarrow | 0.849 \downarrow |
| KGEC | 263 | 0.772 | 0.706 | 0.807 | 0.920 |
| WN18RR | | | | | |
| Uncal | 3437 | 0.223 | 0.014 | 0.401 | 0.528 |
| PS | 3437 | 0.223 | 0.014 | 0.401 | 0.528 |
| HB | 19455 \downarrow | 0.071 \downarrow | 0.053 \uparrow | 0.087 \downarrow | 0.099 \downarrow |
| IR | 18143 \downarrow | 0.102 \downarrow | 0.080 \uparrow | 0.119 \downarrow | 0.139 \downarrow |
| BBQ | 18196 \downarrow | 0.071 \downarrow | 0.050 \uparrow | 0.085 \downarrow | 0.105 \downarrow |
| VS | 3421 \uparrow | 0.224 \uparrow | 0.014 | 0.401 | 0.529 \uparrow |
| MS | 18178 \downarrow | 0.009 \downarrow | 0.003 \downarrow | 0.008 \downarrow | 0.020 \downarrow |
| TS | 3437 | 0.223 | 0.014 | 0.401 | 0.528 |
| Meta-Cal | 3437 | 0.223 | 0.014 | 0.401 | 0.528 |
| PTS | 3437 | 0.223 | 0.014 | 0.401 | 0.528 |
| KGEC | 3437 | 0.223 | 0.014 | 0.401 | 0.528 |
| FB15K | | | | | |
| Uncal | 40 | 0.731 | 0.646 | 0.793 | 0.865 |
| PS | 40 | 0.731 | 0.646 | 0.793 | 0.865 |
| HB | 2275 \downarrow | 0.570 \downarrow | 0.510 \downarrow | 0.614 \downarrow | 0.670 \downarrow |
| IR | 982 \downarrow | 0.615 \downarrow | 0.530 \downarrow | 0.675 \downarrow | 0.761 \downarrow |
| BBQ | 1275 \downarrow | 0.589 \downarrow | 0.509 \downarrow | 0.646 \downarrow | 0.726 \downarrow |
| VS | 41 \downarrow | 0.730 \downarrow | 0.646 | 0.791 \downarrow | 0.862 \downarrow |
| MS | 3687 \downarrow | 0.038 \downarrow | 0.024 \downarrow | 0.039 \downarrow | 0.061 \downarrow |
| TS | 40 | 0.731 | 0.646 | 0.793 | 0.865 |
| Meta-Cal | 1149 \downarrow | 0.677 \downarrow | 0.604 \downarrow | 0.735 \downarrow | 0.787 \downarrow |
| PTS | 40 | 0.731 | 0.646 | 0.793 | 0.865 |
| KGEC | 40 | 0.731 | 0.646 | 0.793 | 0.865 |
| FB15K-237 | | | | | |
| Uncal | 173 | 0.330 | 0.231 | 0.368 | 0.527 |
| PS | 173 | 0.330 | 0.231 | 0.368 | 0.527 |
| HB | 3497 \downarrow | 0.289 \downarrow | 0.224 \downarrow | 0.321 \downarrow | 0.416 \downarrow |
| IR | 2141 \downarrow | 0.309 \downarrow | 0.234 \uparrow | 0.343 \downarrow | 0.455 \downarrow |
| BBQ | 2335 \downarrow | 0.280 \downarrow | 0.209 \downarrow | 0.310 \downarrow | 0.422 \downarrow |
| VS | 173 | 0.330 | 0.231 | 0.368 | 0.527 |
| MS | 3704 \downarrow | 0.033 \downarrow | 0.014 \downarrow | 0.032 \downarrow | 0.070 \downarrow |
| TS | 173 | 0.330 | 0.231 | 0.368 | 0.527 |
| Meta-Cal | 1231 \downarrow | 0.308 \downarrow | 0.218 \downarrow | 0.344 \downarrow | 0.490 \downarrow |
| PTS | 173 | 0.330 | 0.231 | 0.368 | 0.527 |
| KGEC | 173 | 0.330 | 0.231 | 0.368 | 0.527 |

slightly degrades performance on FB15K and PTS on WN18, but given that the decline is minor and it performs well on other datasets, its overall impact remains acceptable.

5.3 Effectiveness Study for RQ2

Table 2 presents the calibration performance of various methods across multiple KGE models and datasets. Notably, baselines such as HB, IR, BBQ, MS, and Meta-Cal are excluded, due to their detrimental impact on ranking performance, as shown in Section 5.2. Since preserving the original ranking order is essential in KGE settings, these calibration methods that degrade ranking performance are considered unsuitable for practical deployment and omitted from further evaluation.

Overall, across all datasets and models, KGEC

¹<https://efs-opensource.github.io/calibration-framework/build/html/index.html>

²<https://torch-uncertainty.github.io>

³<https://github.com/maxc01/metacal/tree/master>

⁴<https://github.com/tochris/pts-uncertainty>

⁵<https://anonymous.4open.science/r/KGE-Calibrator-D780/README.md>

Table 2: Effect of different calibration methods on the performance of various KGE models across multiple datasets. For ECE, ACE, and NLL, lower values indicate better calibration performance.

| ECE | TransE | | | | ComplEx | | | | DistMult | | | | RotatE | | | | Average |
|-------|--------|--------|-------|-----------|---------|--------|-------|-----------|----------|--------|-------|-----------|--------|--------|-------|-----------|---------|
| | WN18 | WN18RR | FB15K | FB15K-237 | WN18 | WN18RR | FB15K | FB15K-237 | WN18 | WN18RR | FB15K | FB15K-237 | WN18 | WN18RR | FB15K | FB15K-237 | |
| Uncal | 0.502 | 0.265 | 0.580 | 0.212 | 0.852 | 0.424 | 0.696 | 0.228 | 0.528 | 0.389 | 0.694 | 0.221 | 0.429 | 0.385 | 0.684 | 0.224 | 0.457 |
| PS | 0.634 | 0.031 | 0.530 | 0.218 | 0.854 | 0.427 | 0.701 | 0.229 | 0.529 | 0.394 | 0.700 | 0.222 | 0.876 | 0.425 | 0.722 | 0.235 | 0.483 |
| VS | 0.706 | 0.014 | 0.646 | 0.231 | 0.852 | 0.424 | 0.697 | 0.228 | 0.528 | 0.389 | 0.695 | 0.215 | 0.944 | 0.413 | 0.739 | 0.239 | 0.498 |
| TS | 0.634 | 0.031 | 0.680 | 0.203 | 0.852 | 0.424 | 0.701 | 0.228 | 0.528 | 0.389 | 0.700 | 0.221 | 0.687 | 0.384 | 0.722 | 0.223 | 0.475 |
| PTS | 0.523 | 0.013 | 0.530 | 0.231 | 0.854 | 0.430 | 0.060 | 0.214 | 0.456 | 0.393 | 0.526 | 0.778 | 0.337 | 0.425 | 0.221 | 0.365 | 0.397 |
| KGEC | 0.171 | 0.280 | 0.459 | 0.150 | 0.838 | 0.418 | 0.678 | 0.189 | 0.446 | 0.383 | 0.683 | 0.178 | 0.467 | 0.307 | 0.466 | 0.094 | 0.388 |

| ACE | TransE | | | | ComplEx | | | | DistMult | | | | RotatE | | | | Average |
|-------|--------|--------|-------|-----------|---------|--------|-------|-----------|----------|--------|-------|-----------|--------|--------|-------|-----------|---------|
| | WN18 | WN18RR | FB15K | FB15K-237 | WN18 | WN18RR | FB15K | FB15K-237 | WN18 | WN18RR | FB15K | FB15K-237 | WN18 | WN18RR | FB15K | FB15K-237 | |
| Uncal | 0.506 | 0.274 | 0.565 | 0.180 | 0.852 | 0.424 | 0.696 | 0.228 | 0.528 | 0.389 | 0.694 | 0.220 | 0.429 | 0.385 | 0.684 | 0.224 | 0.455 |
| PS | 0.628 | 0.033 | 0.530 | 0.217 | 0.854 | 0.427 | 0.701 | 0.229 | 0.529 | 0.394 | 0.700 | 0.222 | 0.876 | 0.425 | 0.722 | 0.235 | 0.483 |
| VS | 0.506 | 0.274 | 0.565 | 0.180 | 0.852 | 0.424 | 0.697 | 0.228 | 0.528 | 0.389 | 0.694 | 0.215 | 0.429 | 0.385 | 0.684 | 0.224 | 0.455 |
| TS | 0.628 | 0.033 | 3.312 | 0.154 | 0.852 | 0.423 | 0.701 | 0.228 | 0.528 | 0.389 | 0.700 | 0.220 | 0.687 | 0.384 | 0.722 | 0.222 | 0.636 |
| PTS | 0.516 | 0.013 | 0.530 | 0.231 | 0.854 | 0.424 | 0.060 | 0.207 | 0.446 | 0.391 | 0.522 | 0.778 | 0.337 | 0.418 | 0.221 | 0.363 | 0.394 |
| KGEC | 0.131 | 0.277 | 0.293 | 0.082 | 0.833 | 0.418 | 0.465 | 0.207 | 0.457 | 0.383 | 0.516 | 0.199 | 0.467 | 0.306 | 0.466 | 0.063 | 0.348 |

| NLL | TransE | | | | ComplEx | | | | DistMult | | | | RotatE | | | | Average |
|-------|--------|--------|-------|-----------|---------|--------|-------|-----------|----------|--------|-------|-----------|--------|--------|-------|-----------|---------|
| | WN18 | WN18RR | FB15K | FB15K-237 | WN18 | WN18RR | FB15K | FB15K-237 | WN18 | WN18RR | FB15K | FB15K-237 | WN18 | WN18RR | FB15K | FB15K-237 | |
| Uncal | 2.891 | 6.582 | 3.911 | 5.396 | 6.892 | 7.815 | 5.954 | 7.513 | 7.447 | 7.858 | 5.919 | 7.705 | 1.376 | 6.145 | 4.090 | 5.750 | 5.828 |
| PS | 3.839 | 7.304 | 3.829 | 5.836 | 8.831 | 8.974 | 7.093 | 8.438 | 9.117 | 9.065 | 7.257 | 8.621 | 3.350 | 7.364 | 4.799 | 6.271 | 6.874 |
| VS | / | / | / | / | 6.892 | 7.814 | 5.952 | 7.510 | 7.446 | 7.857 | 5.916 | 7.692 | 1.376 | / | / | / | 6.495 |
| TS | 3.839 | 7.304 | 1.285 | 4.909 | 6.892 | 7.802 | 7.093 | 7.513 | 7.447 | 7.856 | 7.257 | 7.704 | 2.069 | 6.121 | 4.799 | 5.617 | 5.969 |
| PTS | / | 9.181 | 3.829 | 9.448 | 9.314 | 9.171 | 1.906 | 5.714 | / | 9.496 | 4.847 | / | / | / | / | / | 6.990 |
| KGEC | 2.462 | 5.965 | 2.536 | 2.889 | 4.350 | 6.965 | 1.357 | 2.911 | 2.843 | 7.119 | 1.319 | 3.106 | 1.036 | 4.698 | 2.033 | 2.743 | 3.396 |

consistently achieves the lowest average ECE, ACE, and NLL, clearly outperforming all competitive baselines. Key findings from Table 2 include: (1) Limited effectiveness of simple baselines: PS, VS, and TS often perform worse than the uncalibrated models. Their poor performance is likely due to their low model capacity, which is insufficient to capture complex calibration patterns in high-cardinality KGE settings. (2) Improved results with PTS: PTS shows marked improvement over simple baselines by predicting temperature parameters adaptively using a neural network. This flexibility enables better handling of distributional variation, leading to improved calibration performance. (3) Superior performance of KGEC: KGEC achieves the best overall results across all metrics and datasets. Its combination of Jump Selection Strategy, Multi-Binning Scaling, and Wasserstein distance-based loss function effectively addresses the challenges of KGE calibration while preserving ranking quality.

5.4 Efficiency Study for RQ3

Table 5 and Table 6 report the training time and memory usage of different calibration methods across multiple KGE models and datasets. All methods are evaluated on CPU-only environments to ensure fair comparison.

Key Observations from these two tables: (1) KGEC is the most efficient model in both training time and memory usage, consistently outperforming all baseline methods. (2) VS and TS exhibit comparable efficiency, with slightly longer training times than KGEC, which can be attributed to their

simple parametric structures. (3) PTS incurs significantly higher computational costs, both in time and memory, despite its strong calibration performance. This high overhead may limit its applicability in large-scale or resource-constrained scenarios. (4) PS is the slowest method, largely due to the immense number of classes in KGE settings, which makes binary logistic regression computationally expensive.

5.5 Ablation Study, Sensitivity Analysis, and Case Study

Due to space limitations, additional experiments, including the ablation study, sensitivity analysis, and case study, are provided in the Appendix. Please refer to Appendix D, E, and F for details.

6 Conclusion

In this paper, we propose KGEC, the first probability calibration method specifically designed for KGE models. KGEC integrates a Wasserstein distance-based loss function, a multi-binning scaling module, and a jump selection strategy to effectively calibrate the predictive probabilities of KGE models without sacrificing ranking performance. Comprehensive experiments across multiple KGE models and benchmark datasets demonstrate that KGEC significantly outperforms existing calibration baselines in terms of effectiveness and efficiency. Overall, KGEC establishes a strong and efficient foundation for trustworthy link prediction. Future work may explore its applicability to dynamic knowledge graphs or integrating it with uncertainty-aware reasoning systems.

Limitations

While KGEC achieves strong performance in calibrating probability estimates for KGE models, several limitations remain:

(1) Limited Exploration of Expit Transformation Functions. In this work, we adopt the Softmax function as the expit transformation, as our primary focus is on the calibration method itself. However, alternative approaches, such as NIC (Wang et al., 2021) and min-max normalization (Rao, 2021), may further improve performance and merit exploration in future work.

(2) Task-Specific Calibration Considerations. KGEC is optimized for static entity prediction tasks in knowledge graphs. Its effectiveness in other KGE-based applications, such as multi-hop reasoning, fact verification, or temporal/dynamic KG settings, remains untested. These tasks may require adaptation or redesign of the calibration strategy to accommodate different data characteristics and evaluation protocols.

(3) Limited Evaluation Across Advanced KGE Architectures. While KGEC has been extensively evaluated on several representative KGE models (e.g., TransE, DistMult, ComplEx, and RotatE), its generalization to more complex architectures, such as hyperbolic embeddings, graph neural networks, or transformer-based KGE models, has not yet been studied. Extending KGEC to these settings poses challenges in modeling and scalability, and is an important direction for future work.

References

- Hongjoon Ahn, Sungmin Cha, Donggyu Lee, and Taesup Moon. 2019. Uncertainty-based continual learning with adaptive regularization. *NeurIPS*, 32.
- Kurt Bollacker, Colin Evans, Praveen Paritosh, Tim Sturge, and Jamie Taylor. 2008. Freebase: a collaboratively created graph database for structuring human knowledge. In *SIGMOD*, pages 1247–1250.
- Antoine Bordes, Nicolas Usunier, Alberto Garcia-Durán, Jason Weston, and Oksana Yakhnenko. 2013. Translating embeddings for modeling multi-relational data. In *NeurIPS*, pages 2787–2795.
- Marco Cuturi. 2013. Sinkhorn distances: Lightspeed computation of optimal transport. In *NeurIPS*, volume 26.
- Tim Dettmers, Pasquale Minervini, Pontus Stenetorp, and Sebastian Riedel. 2018. Convolutional 2d knowledge graph embeddings. In *AAAI*, volume 32.
- Yarin Gal and Zoubin Ghahramani. 2016. Dropout as a bayesian approximation: Representing model uncertainty in deep learning. In *ICML*, pages 1050–1059. PMLR.
- Chuan Guo, Geoff Pleiss, Yu Sun, and Kilian Q Weinberger. 2017. On calibration of modern neural networks. In *ICML*, pages 1321–1330. PMLR.
- Alex Krizhevsky et al. 2009. Learning multiple layers of features from tiny images.
- Meelis Kull, Telmo Silva Filho, and Peter Flach. 2017. Beta calibration: a well-founded and easily implemented improvement on logistic calibration for binary classifiers. In *Artificial intelligence and statistics*, pages 623–631. PMLR.
- Balaji Lakshminarayanan, Alexander Pritzel, and Charles Blundell. 2017. Simple and scalable predictive uncertainty estimation using deep ensembles. *NeurIPS*, 30.
- Jens Lehmann, Robert Isele, Max Jakob, Anja Jentzsch, Dimitris Kontokostas, Pablo Mendes, Sebastian Hellmann, Mohamed Morsey, Patrick van Kleef, Sören Auer, and Chris Bizer. 2015. DBpedia - a large-scale, multilingual knowledge base extracted from wikipedia. *Semantic Web Journal*, 6(2):167–195.
- Lihui Liu, Boxin Du, Yi Ren Fung, Heng Ji, Jiejun Xu, and Hanghang Tong. 2021. Kompare: a knowledge graph comparative reasoning system. In *SIGKDD*, pages 3308–3318.
- Ilya Loshchilov and Frank Hutter. 2019. [Decoupled weight decay regularization](#). In *ICLR*.
- Xingchen Ma and Matthew B Blaschko. 2021. Metacal: Well-controlled post-hoc calibration by ranking. In *ICML*, pages 7235–7245. PMLR.
- Xianghui Meng, Yang Song, Qingchun Bai, and Taoyi Wang. 2023. Cbki: A confidence-based knowledge integration framework for multi-choice machine reading comprehension. *Knowledge-Based Systems*, 277:110796.
- George A Miller. 1995. Wordnet: a lexical database for english. *Communications of the ACM*, 38(11):39–41.
- Sameh K Mohamed, Vít Nováček, and Aayah Nounu. 2020. Discovering protein drug targets using knowledge graph embeddings. *Bioinformatics*, 36(2):603–610.
- Mahdi Pakdaman Naeini, Gregory Cooper, and Milos Hauskrecht. 2015. Obtaining well calibrated probabilities using bayesian binning. In *AAAI*, volume 29.
- Maximilian Nickel, Kevin Murphy, Volker Tresp, and Evgeniy Gabrilovich. 2015. A review of relational machine learning for knowledge graphs. *Proceedings of the IEEE*, 104(1):11–33.

| | | | |
|-----|---|--|-----|
| 754 | Jeremy Nixon, Michael W Dusenberry, Linchuan Zhang, | Kristina Toutanova and Danqi Chen. 2015. Observed | 805 |
| 755 | Ghassen Jerfel, and Dustin Tran. 2019. Measuring | versus latent features for knowledge base and text | 806 |
| 756 | calibration in deep learning. In <i>CVPR workshops</i> , | inference. In <i>Proceedings of the 3rd workshop on</i> | 807 |
| 757 | volume 2. | <i>continuous vector space models and their composi-</i> | 808 |
| | | <i>tionality</i> , pages 57–66. | 809 |
| 758 | Pouya Pezeshkpour, Yifan Tian, and Sameer Singh. | | |
| 759 | 2020. Revisiting evaluation of knowledge base com- | Théo Trouillon, Johannes Welbl, Sebastian Riedel, Éric | 810 |
| 760 | pletion models. <i>AKBC</i> . | Gaussier, and Guillaume Bouchard. 2016. Complex | 811 |
| | | embeddings for simple link prediction. In <i>ICML</i> , | 812 |
| 761 | John Platt et al. 1999. Probabilistic outputs for support | pages 2071–2080. | 813 |
| 762 | vector machines and comparisons to regularized like- | | |
| 763 | lihood methods. <i>Advances in large margin classifiers</i> , | Kai Wang, Yu Liu, and Quan Z Sheng. 2021. Neighbor- | 814 |
| 764 | 10(3):61–74. | hood intervention consistency: Measuring confidence | 815 |
| | | for knowledge graph link prediction. In <i>IJCAI</i> , pages | 816 |
| 765 | ZAishwarya Rao. 2021. Calibrating knowledge graphs. | 2090–2096. | 817 |
| 766 | In <i>Rochester Institute of Technology</i> . | | |
| 767 | Tara Safavi, Danai Koutra, and Edgar Meij. 2020. Evalu- | Chenyan Xiong, Russell Power, and Jamie Callan. 2017. | 818 |
| 768 | ating the calibration of knowledge graph embeddings | Explicit semantic ranking for academic search via | 819 |
| 769 | for trustworthy link prediction. In <i>EMNLP</i> , pages | knowledge graph embedding. In <i>WWW</i> , pages 1271– | 820 |
| 770 | 8308–8321. | 1279. | 821 |
| | | | |
| 771 | Tao Shen, Xiubo Geng, Tao Qin, Daya Guo, Duyu | An Yang, Quan Wang, Jing Liu, Kai Liu, Yajuan Lyu, | 822 |
| 772 | Tang, Nan Duan, Guodong Long, and Daxin Jiang. | Hua Wu, Qiaoqiao She, and Sujian Li. 2019. Enhanc- | 823 |
| 773 | 2019. Multi-task learning for conversational ques- | ing pre-trained language representations with rich | 824 |
| 774 | tion answering over a large-scale knowledge base. In | knowledge for machine reading comprehension. In | 825 |
| 775 | <i>EMNLP-IJCNLP</i> , pages 2442–2451. | <i>ACL</i> , pages 2346–2357. | 826 |
| | | | |
| 776 | Wei Shen, Yang Yang, and Yinan Liu. 2022. Multi-view | Bishan Yang, Scott Wen-tau Yih, Xiaodong He, Jianfeng | 827 |
| 777 | clustering for open knowledge base canonicalization. | Gao, and Li Deng. 2015. Embedding entities and | 828 |
| 778 | In <i>SIGKDD</i> , pages 1578–1588. | relations for learning and inference in knowledge | 829 |
| | | bases. In <i>ICLR</i> . | 830 |
| 779 | Richard Socher, Alex Perelygin, Jean Wu, Jason | Qichen Ye, Bowen Cao, Nuo Chen, Weiyuan Xu, and | 831 |
| 780 | Chuang, Christopher D Manning, Andrew Y Ng, and | Yuexian Zou. 2023. Fits: Fine-grained two-stage | 832 |
| 781 | Christopher Potts. 2013. Recursive deep models for | training for knowledge-aware question answering. In | 833 |
| 782 | semantic compositionality over a sentiment treebank. | <i>AAAI</i> , volume 37, pages 13914–13922. | 834 |
| 783 | In <i>EMNLP</i> , pages 1631–1642. | | |
| | | | |
| 784 | Fabian M. Suchanek, Gjergji Kasneci, and Gerhard | Bianca Zadrozny and Charles Elkan. 2001. Obtaining | 835 |
| 785 | Weikum. 2007. Yago: a core of semantic knowledge. | calibrated probability estimates from decision trees | 836 |
| 786 | In <i>WWW</i> , pages 697–706. | and naive bayesian classifiers. In <i>ICML</i> , pages 609– | 837 |
| | | 616. | 838 |
| 787 | Zequan Sun, Wei Hu, Qingheng Zhang, and Yuzhong Qu. | Bianca Zadrozny and Charles Elkan. 2002. Transform- | 839 |
| 788 | 2018. Bootstrapping entity alignment with knowl- | ing classifier scores into accurate multiclass probab- | 840 |
| 789 | edge graph embedding. In <i>IJCAI</i> , volume 18. | ility estimates. In <i>SIGKDD</i> , pages 694–699. | 841 |
| | | | |
| 790 | Zhiqing Sun, Zhi-Hong Deng, Jian-Yun Nie, and Jian | Xiangxiang Zeng, Xinqi Tu, Yuansheng Liu, Xi- | 842 |
| 791 | Tang. 2019. Rotate: Knowledge graph embedding by | angzheng Fu, and Yansen Su. 2022. Toward bet- | 843 |
| 792 | relational rotation in complex space. In <i>ICLR</i> . | ter drug discovery with knowledge graph. <i>Current</i> | 844 |
| | | <i>opinion in structural biology</i> , 72:114–126. | 845 |
| 793 | Pedro Tabacof and Luca Costabello. 2020. Probability | Ruiqi Zhu, Fangrong Wang, Alan Bundy, Xue Li, | 846 |
| 794 | calibration for knowledge graph embedding models. | Kwabena Nuamah, Lei Xu, Stefano Mauceri, and | 847 |
| 795 | In <i>ICLR</i> . | Jeff Z Pan. 2022. A closer look at probability cali- | 848 |
| | | bration of knowledge graph embedding. In <i>IJCKG</i> , | 849 |
| 796 | Sunil Thulasidasan, Gopinath Chennupati, Jeff A | pages 104–109. | 850 |
| 797 | Bilmes, Tanmoy Bhattacharya, and Sarah Michal- | | |
| 798 | lak. 2019. On mixup training: Improved calibration | | |
| 799 | and predictive uncertainty for deep neural networks. | | |
| 800 | <i>NeurIPS</i> , 32. | | |
| | | | |
| 801 | Christian Tomani, Daniel Cremers, and Florian Buet- | A Score functions of popular KGE | 851 |
| 802 | ner. 2022. Parameterized temperature scaling for | models | 852 |
| 803 | boosting the expressive power in post-hoc uncertainty | For popular KGE models, we show the score func- | 853 |
| 804 | calibration. In <i>ECCV</i> , pages 555–569. Springer. | tions of them in Table 3. | 854 |

Table 3: Score functions of popular KGE models, where $\|\cdot\|$ denotes the L_1 norm, $\langle \cdot \rangle$ denotes the generalized dot product, \mathbf{t}^* denotes the complex conjugate of \mathbf{t} , Re refers to the real part of a complex number, and \circ denotes the Hadamard product.

| KGE model | Score function |
|----------------------------------|--|
| TransE (Bordes et al., 2013) | $-\ \mathbf{h} + \mathbf{r} - \mathbf{t}\ $ |
| DistMult (Yang et al., 2015) | $\langle \mathbf{r}, \mathbf{h}, \mathbf{t} \rangle$ |
| ComplEx (Trouillon et al., 2016) | $Re(\langle \mathbf{r}, \mathbf{h}, \mathbf{t}^* \rangle)$ |
| RotatE (Sun et al., 2019) | $-\ \mathbf{h} \circ \mathbf{r} - \mathbf{t}\ $ |

B Handling Zero Probabilities in KL Divergence

Let p and q be two discrete probability distributions over a finite set \mathcal{X} . The Kullback–Leibler (KL) divergence from q to p is defined as:

$$D_{\text{KL}}(p \parallel q) = \sum_{x \in \mathcal{X}} p(x) \log \frac{p(x)}{q(x)}.$$

While this expression is well-defined when both $p(x) > 0$ and $q(x) > 0$, edge cases involving zero probabilities require special attention. Below, we analyze two important cases.

Case 1: $p(x) = 0$

When $p(x) = 0$, the corresponding term in the summation becomes:

$$0 \cdot \log \frac{0}{q(x)}.$$

Although $\log 0$ is undefined, this term is conventionally set to zero. This is justified by the limit:

$$\lim_{u \rightarrow 0^+} u \log \frac{u}{q(x)} = 0.$$

Hence, for numerical stability and analytical consistency, we define:

$$p(x) \log \frac{p(x)}{q(x)} = 0 \quad \text{when } p(x) = 0.$$

Case 2: $q(x) = 0$ and $p(x) > 0$

This case is more problematic. If $p(x) > 0$ and $q(x) = 0$, the logarithmic term becomes:

$$\log \frac{p(x)}{q(x)} = +\infty,$$

which leads to:

$$p(x) \log \frac{p(x)}{q(x)} = +\infty.$$

Thus, the KL divergence is undefined (i.e., infinite) in this case. Formally:

$$D_{\text{KL}}(p \parallel q) = +\infty$$

if $\exists x \in \mathcal{X}$ such that $p(x) > 0$ and $q(x) = 0$.

Table 4: Statistics of the used KGE datasets.

| dataset | #Entity | #Relation | #Training | #Validation | #Testing |
|-----------|---------|-----------|-----------|-------------|----------|
| WN18 | 40,943 | 18 | 141,442 | 5,000 | 5,000 |
| WN18RR | 40,943 | 11 | 86,835 | 3,034 | 3,134 |
| FB15K | 14,951 | 1,345 | 483,142 | 50,000 | 59,071 |
| FB15K-237 | 14,541 | 237 | 272,115 | 17,535 | 20,466 |

Summary

Each term $p(x) \log \frac{p(x)}{q(x)}$ in the KL divergence is interpreted as follows:

- If $p(x) = 0$, the term is defined as 0 (by convention via limiting argument).
- If $p(x) > 0$ and $q(x) = 0$, the term is $+\infty$, causing the entire divergence to diverge.

Thus, the KL divergence is finite if and only if the support of p is a subset of the support of q :

$$D_{\text{KL}}(p \parallel q) = \begin{cases} \sum_x p(x) \log \frac{p(x)}{q(x)}, & \text{if } q(x) > 0 \\ +\infty, & \text{otherwise.} \end{cases}$$

This behavior makes KL divergence highly sensitive to support mismatch. In high-cardinality tasks such as entity prediction in KGs, sparse output distributions and zero-valued targets frequently occur. This can cause instability during training, particularly in gradient-based optimization, and may compromise calibration performance if not handled appropriately.

C Statistics of the used KGE datasets

The statistics of the used KGE datasets are summarized into Table 4.

D Ablation Study

To assess the individual contribution of each component in KGEC, we perform a comprehensive ablation study across five key metrics: ECE, ACE, NLL, training time, and memory usage. Figure 2 reports the average performance across all datasets and KGE models, providing an overall comparison of model variants. Detailed experimental results for each component on individual datasets and KGE models are presented in Table 11.

We evaluate the following four variants: (1) KGEC: The full model, incorporating all components—Jump Selection Strategy (JSS), Multi-Binning Scaling (MBS), and the Wasserstein distance-based loss. (2) KGEC-loss: Replaces the Wasserstein loss with KL divergence while retaining JSS and MBS. (3) KGEC-loss-MBS: Further

Table 5: Training time in seconds taken to calibrate entity prediction using different methods. Best and second-ranked results are in bold and underlined, respectively. For fair comparison, these results are obtained using CPU only.

| Method | TransE | | | | ComplEx | | | | DistMult | | | | RotatE | | | | Average |
|--------|-----------|-----------|-----------|-----------|-----------|-----------|-----------|-----------|-----------|-----------|-----------|-----------|-----------|-----------|-----------|-----------|--------------|
| | WN18 | WN18RR | FB15K | FB15K-237 | WN18 | WN18RR | FB15K | FB15K-237 | WN18 | WN18RR | FB15K | FB15K-237 | WN18 | WN18RR | FB15K | FB15K-237 | |
| PS | 50551.471 | 32130.612 | 66566.552 | 22756.968 | 44484.280 | 27740.023 | 66631.859 | 20060.975 | 48902.412 | 31739.057 | 58074.230 | 21682.032 | 46162.422 | 30198.810 | 65506.688 | 20522.725 | 40856.945 |
| VS | 2.857 | 1.893 | 25.357 | 3.493 | 2.661 | 1.620 | 16.228 | 3.218 | 4.114 | 1.914 | 20.779 | 3.456 | 2.656 | 1.706 | 25.995 | 3.277 | <u>2.527</u> |
| TS | 5.235 | 3.207 | 20.037 | 6.475 | 5.063 | 3.121 | 18.825 | 6.276 | 5.180 | 3.204 | 19.734 | 6.412 | 5.456 | 3.171 | 20.646 | 6.345 | 8.649 |
| PTS | 3452.440 | 2123.849 | 16769.166 | 5856.000 | 3432.436 | 2122.273 | 16510.019 | 5764.345 | 3450.331 | 2120.555 | 16898.528 | 5868.468 | 3425.148 | 2113.001 | 16802.984 | 5853.287 | 7035.177 |
| KGEC | 2.727 | 1.776 | 10.873 | 3.602 | 2.698 | 1.727 | 10.560 | 3.624 | 2.741 | 1.696 | 10.645 | 3.705 | 2.662 | 1.658 | 10.758 | 4.003 | 4.716 |

Table 6: Memory usage in MBs taken to calibrate entity prediction using different methods. Best and second-ranked results are in bold and underlined, respectively. For fair comparison, these results are obtained using CPU only.

| Method | TransE | | | | ComplEx | | | | DistMult | | | | RotatE | | | | Average |
|--------|----------|----------|-----------|-----------|----------|----------|-----------|-----------|----------|----------|-----------|-----------|----------|----------|-----------|-----------|---------------|
| | WN18 | WN18RR | FB15K | FB15K-237 | WN18 | WN18RR | FB15K | FB15K-237 | WN18 | WN18RR | FB15K | FB15K-237 | WN18 | WN18RR | FB15K | FB15K-237 | |
| PS | 1564.336 | 950.762 | 5706.102 | 1948.508 | 1566.598 | 950.270 | 5706.832 | 1948.664 | 1565.820 | 949.633 | 5705.828 | 1947.574 | 1566.477 | 950.793 | 5706.875 | 1948.371 | 2542.715 |
| VS | 84.477 | 84.383 | 86.098 | 84.348 | 82.059 | 83.152 | 86.918 | 80.770 | 83.609 | 83.883 | 80.883 | 81.320 | 80.570 | 83.145 | 86.152 | 80.941 | 83.294 |
| TS | 1562.625 | 948.453 | 5703.750 | 1947.629 | 1562.984 | 949.285 | 5703.047 | 1945.566 | 1562.340 | 948.504 | 5704.801 | 1945.828 | 1562.914 | 948.566 | 5703.359 | 1944.730 | 2540.274 |
| PTS | 6655.574 | 7017.359 | 11154.340 | 9554.723 | 6804.816 | 7022.313 | 10185.500 | 9629.871 | 6957.012 | 6696.055 | 10180.105 | 9407.988 | 7047.270 | 7074.051 | 10521.520 | 8659.395 | 8410.493 |
| KGEC | 30.484 | 28.289 | 7.570 | 15.273 | 26.652 | 32.176 | 9.535 | 15.285 | 34.316 | 32.047 | 10.531 | 13.492 | 34.320 | 32.191 | 7.551 | 16.930 | 21.665 |

removes MBS, retaining only JSS and KL divergence. (4) KGEC-loss-MBS-JSS: The base version using only KL divergence, without any of the proposed enhancements.

Key Observations: (1) Full Model Superiority: KGEC achieves the best performance across all five metrics. It yields the lowest calibration errors ($ECE = 0.388$, $ACE = 0.348$, $NLL = 3.396$) while maintaining high efficiency (training time = 4.716s, memory usage = 21.665MB). (2) Impact of Wasserstein Loss: Comparing KGEC to KGEC-loss reveals substantial calibration improvements, validating the advantage of using Wasserstein distance over KL divergence in high-cardinality, ranking-sensitive KGE settings. This supports our hypothesis that the Wasserstein-based objective is better suited to the probability distribution landscape of KGE. (3) Effect of MBS: Removing MBS (KGEC-loss vs. KGEC-loss-MBS) degrades ECE (from 0.450 to 0.487) and NLL (from 4.960 to 5.590), indicating that MBS enhances calibration by modeling probability intervals more effectively. Interestingly, ACE improves after removing MBS. This anomaly may arise because the KL divergence used in KGEC-loss amplifies ACE more than expected, suggesting ACE is especially sensitive to the choice of loss function. (4) Efficiency Gain from JSS: While KGEC-loss-MBS and KGEC-loss-MBS-JSS exhibit similar calibration performance, the inclusion of JSS dramatically reduces training time (from 65.871s to 4.659s) and memory usage (from 97.608MB to 20.032MB), confirming JSS’s effectiveness in improving computational efficiency.

Overall, all three components are essential for balancing calibration performance and computational cost. MBS and Wasserstein loss enhance

calibration performance, while JSS ensures scalability. The full KGEC model delivers the strongest overall performance.

E Sensitivity Analysis

To assess the robustness and stability of our proposed KGEC method, we conduct a comprehensive sensitivity analysis by varying three critical hyperparameters: the number of bins, the initial temperature, and the learning rate. We evaluate the impact of each parameter on three calibration metrics, i.e., ECE, ACE, and NLL, across all KGE models and datasets. Results are summarized in Tables 12, 13, and 14.

Effect of the Number of Bins. We vary the number of bins from 1 to 20. Table 12 shows that using only one bin (equivalent to vanilla temperature scaling) results in poor performance across all metrics, highlighting its limited flexibility. As the number of bins increases, KGEC becomes more expressive and better calibrated. The best average performance is observed at 19 bins ($ECE = 0.352$, $ACE = 0.343$, $NLL = 3.361$), though results are stable within the 10–20 bin range. This confirms the importance of multi-binning for modeling diverse score distributions, while also indicating that KGEC is robust to bin selection within a reasonable interval.

Effect of Initial Temperature. We examine initial temperature values ranging from 0 to 2.0. As shown in Table 13, extreme initializations (e.g., 0.0 or 2.0) lead to degraded performance due to optimization instability. An initial temperature of 1.0 yields the best results ($ECE = 0.388$, $ACE = 0.348$, $NLL = 3.396$), aligning with standard practice in temperature scaling (Guo et al., 2017). The results

Table 7: Summary table for calibration method used by related works.

| Calibration method | Parametric method | Used works |
|--|-------------------|---|
| Isotonic Regression (Zadrozny and Elkan, 2002) | No | (Tabacof and Costabello, 2020), (Wang et al., 2021), (Zhu et al., 2022) |
| Histogram Binning (Zadrozny and Elkan, 2001) | No | (Zhu et al., 2022) |
| Beta Calibration (Kull et al., 2017) | Yes | (Zhu et al., 2022) |
| Platt Scaling (Platt et al., 1999) | Yes | (Tabacof and Costabello, 2020), (Wang et al., 2021), (Zhu et al., 2022) |
| Matrix Scaling (Guo et al., 2017) | Yes | (Safavi et al., 2020) |
| Vector Scaling (Guo et al., 2017) | Yes | (Safavi et al., 2020) |
| Temperature Scaling (Guo et al., 2017) | Yes | (Zhu et al., 2022) |

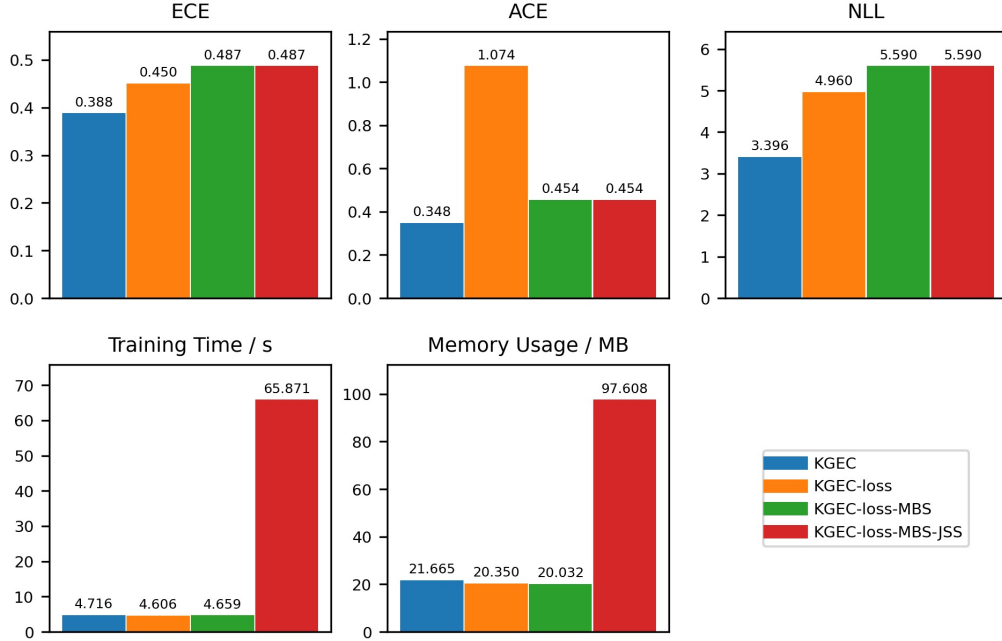


Figure 2: Ablation study of KGEC components across five evaluation metrics: ECE, ACE, NLL, training time (seconds), and memory usage (MB). Lower values indicate better performance.

indicate that KGEC is relatively insensitive to this hyperparameter, as long as it is initialized within a moderate range.

Effect of Learning Rate. Table 14 presents results under learning rates ranging from 0.001 to 0.1. We find that too small learning rates (e.g., 0.001) may underfit the calibration model, while overly large values (e.g., 0.1) can cause instability and degraded performance. The learning rate of 0.01 achieves the best overall calibration (ECE = 0.388, ACE = 0.348, NLL = 3.396), striking a balance between convergence speed and stability.

Summary. Across all experiments, KGEC demonstrates strong robustness to hyperparameter variations. The best performance is consistently achieved with moderate hyperparameter values: a bin count between 10 and 20, an initial temperature near 1.0, and a learning rate around 0.01. These findings suggest that KGEC is both stable and practical, requiring minimal hyperparameter tuning for

| Query: (Greece, _member_of_domain_region, ?) | | |
|--|---------------------|--------------------------|
| True answer: sibyl | | |
| Ranked candidate entities | Uncalibrated scores | Calibrated probabilities |
| Greece | -0.1873 | 0.0302 |
| Holy_See | -0.2946 | 0.0272 |
| sibyl | -0.5992 | 0.0200 |
| Colosseum | -0.8017 | 0.0164 |
| Sistine_Chapel | -0.8683 | 0.0153 |
| Roman | -1.1427 | 0.0116 |
| Italy | -1.1464 | 0.0116 |
| Rome | -1.1873 | 0.0111 |
| Seven_Hills_of_Rome | -1.3174 | 0.0098 |
| augur | -1.3962 | 0.0090 |

Figure 3: Case 1 from the WN18RR dataset using the TransE model.

optimal performance across diverse KGE models and datasets.

F Case Study

To illustrate the practical benefits of KGEC calibration, we present two representative case studies from the WN18RR dataset using the TransE

Table 8: Effect of different calibration methods on the performance of the ComplEx model across various datasets.

| Method | MR | MRR | HITS@1 | HITS@3 | HITS@10 |
|------------------|---------|---------|---------|---------|---------|
| WN18 | | | | | |
| Uncal | 311 | 0.893 | 0.854 | 0.925 | 0.953 |
| PS | 311 | 0.893 | 0.854 | 0.925 | 0.953 |
| HB | 14328 ↓ | 0.274 ↓ | 0.262 ↓ | 0.285 ↓ | 0.289 ↓ |
| IR | 14094 ↓ | 0.290 ↓ | 0.280 ↓ | 0.298 ↓ | 0.304 ↓ |
| BBQ | 13657 ↓ | 0.236 ↓ | 0.194 ↓ | 0.271 ↓ | 0.306 ↓ |
| VS | 305 ↑ | 0.893 | 0.854 | 0.925 | 0.953 |
| MS | 16825 ↓ | 0.011 ↓ | 0.004 ↓ | 0.012 ↓ | 0.022 ↓ |
| TS | 311 | 0.893 | 0.854 | 0.925 | 0.953 |
| Meta-Cal | 1260 ↓ | 0.851 ↓ | 0.813 ↓ | 0.880 ↓ | 0.908 ↓ |
| PTS | 311 | 0.893 | 0.854 | 0.925 | 0.953 |
| KGEC | 311 | 0.893 | 0.854 | 0.925 | 0.953 |
| WN18RR | | | | | |
| Uncal | 5469 | 0.469 | 0.428 | 0.486 | 0.552 |
| PS | 5469 | 0.469 | 0.428 | 0.486 | 0.552 |
| HB | 18836 ↓ | 0.107 ↓ | 0.100 ↓ | 0.112 ↓ | 0.118 ↓ |
| IR | 18244 ↓ | 0.103 ↓ | 0.090 ↓ | 0.110 ↓ | 0.124 ↓ |
| BBQ | 18200 ↓ | 0.087 ↓ | 0.076 ↓ | 0.097 ↓ | 0.105 ↓ |
| VS | 5447 ↑ | 0.469 | 0.428 | 0.486 | 0.552 |
| MS | 18191 ↓ | 0.009 ↓ | 0.003 ↓ | 0.009 ↓ | 0.020 ↓ |
| TS | 5469 | 0.469 | 0.428 | 0.486 | 0.552 |
| Meta-Cal | 6416 ↓ | 0.445 ↓ | 0.407 ↓ | 0.459 ↓ | 0.522 |
| PTS | 5469 | 0.469 | 0.428 | 0.486 | 0.552 |
| KGEC | 5469 | 0.469 | 0.428 | 0.486 | 0.552 |
| FB15K | | | | | |
| Uncal | 45 | 0.770 | 0.703 | 0.816 | 0.885 |
| PS | 45 | 0.770 | 0.703 | 0.816 | 0.885 |
| HB | 1747 ↓ | 0.610 ↓ | 0.543 ↓ | 0.661 ↓ | 0.724 ↓ |
| IR | 970 ↓ | 0.652 ↓ | 0.579 ↓ | 0.704 ↓ | 0.780 ↓ |
| BBQ | 797 ↓ | 0.597 ↓ | 0.509 ↓ | 0.656 ↓ | 0.757 ↓ |
| VS | 43 ↑ | 0.770 | 0.703 | 0.816 | 0.885 ↑ |
| MS | 3693 ↓ | 0.025 ↓ | 0.010 ↓ | 0.024 ↓ | 0.055 ↓ |
| TS | 45 | 0.770 | 0.703 | 0.816 | 0.885 |
| Meta-Cal | 484 ↓ | 0.715 ↓ | 0.651 ↓ | 0.759 ↓ | 0.826 ↓ |
| PTS | 45 | 0.770 | 0.703 | 0.816 | 0.885 |
| KGEC | 45 | 0.770 | 0.703 | 0.816 | 0.885 |
| FB15K-237 | | | | | |
| Uncal | 166 | 0.322 | 0.230 | 0.352 | 0.511 |
| PS | 166 | 0.322 | 0.230 | 0.352 | 0.511 |
| HB | 2882 ↓ | 0.274 ↓ | 0.201 ↓ | 0.305 ↓ | 0.420 ↓ |
| IR | 2185 ↓ | 0.296 ↓ | 0.220 ↑ | 0.328 ↓ | 0.449 ↓ |
| BBQ | 1661 ↓ | 0.249 ↓ | 0.176 ↓ | 0.273 ↓ | 0.399 ↓ |
| VS | 166 | 0.322 | 0.230 | 0.352 | 0.512 ↑ |
| MS | 3704 ↓ | 0.033 ↓ | 0.014 ↓ | 0.032 ↓ | 0.070 ↓ |
| TS | 166 | 0.322 | 0.230 | 0.352 | 0.511 |
| Meta-Cal | 267 ↓ | 0.310 ↓ | 0.218 ↓ | 0.339 ↓ | 0.498 ↓ |
| PTS | 166 | 0.322 | 0.230 | 0.352 | 0.511 |
| KGEC | 166 | 0.322 | 0.230 | 0.352 | 0.511 |

Table 9: Effect of different calibration methods on the performance of the DistMult model across various datasets.

| Method | MR | MRR | HITS@1 | HITS@3 | HITS@10 |
|------------------|---------|---------|---------|---------|---------|
| WN18 | | | | | |
| Uncal | 227 | 0.685 | 0.529 | 0.829 | 0.933 |
| PS | 227 | 0.685 | 0.529 | 0.829 | 0.933 |
| HB | 14718 ↓ | 0.240 ↓ | 0.216 ↓ | 0.262 ↓ | 0.271 ↓ |
| IR | 14271 ↓ | 0.260 ↓ | 0.237 ↓ | 0.279 ↓ | 0.294 ↓ |
| BBQ | 13614 ↓ | 0.201 ↓ | 0.154 ↓ | 0.232 ↓ | 0.293 ↓ |
| VS | 224 ↑ | 0.685 | 0.529 | 0.829 | 0.933 |
| MS | 16984 ↓ | 0.011 ↓ | 0.004 ↓ | 0.012 ↓ | 0.022 ↓ |
| TS | 227 | 0.685 | 0.529 | 0.829 | 0.933 |
| Meta-Cal | 770 ↓ | 0.663 ↓ | 0.508 ↓ | 0.805 ↓ | 0.908 ↓ |
| PTS | 240 ↓ | 0.685 | 0.529 | 0.829 | 0.932 ↓ |
| KGEC | 227 | 0.685 | 0.529 | 0.829 | 0.933 |
| WN18RR | | | | | |
| Uncal | 4912 | 0.439 | 0.394 | 0.453 | 0.532 |
| PS | 4909 ↑ | 0.439 | 0.394 | 0.453 | 0.532 |
| HB | 19006 ↓ | 0.100 ↓ | 0.090 ↑ | 0.108 ↓ | 0.117 ↓ |
| IR | 18174 ↓ | 0.099 ↓ | 0.083 ↑ | 0.109 ↓ | 0.124 ↓ |
| BBQ | 18192 ↓ | 0.088 ↓ | 0.073 ↑ | 0.100 ↓ | 0.109 ↓ |
| VS | 4888 ↑ | 0.439 | 0.394 | 0.453 | 0.532 |
| MS | 18172 ↓ | 0.009 ↓ | 0.003 ↓ | 0.009 ↓ | 0.020 ↓ |
| TS | 4909 ↑ | 0.439 | 0.394 | 0.453 | 0.532 |
| Meta-Cal | 6157 ↓ | 0.406 ↓ | 0.366 ↓ | 0.419 ↓ | 0.493 ↓ |
| PTS | 4909 ↑ | 0.439 | 0.394 | 0.453 | 0.532 |
| KGEC | 4909 ↑ | 0.439 | 0.394 | 0.453 | 0.532 |
| FB15K | | | | | |
| Uncal | 41 | 0.768 | 0.701 | 0.813 | 0.884 |
| PS | 41 | 0.768 | 0.701 | 0.813 | 0.884 |
| HB | 1528 ↓ | 0.630 ↓ | 0.562 ↓ | 0.679 ↓ | 0.748 ↓ |
| IR | 952 ↓ | 0.667 ↓ | 0.599 ↓ | 0.713 ↓ | 0.787 ↓ |
| BBQ | 692 ↓ | 0.603 ↓ | 0.512 ↓ | 0.659 ↓ | 0.775 ↓ |
| VS | 39 ↑ | 0.768 | 0.701 | 0.814 ↑ | 0.885 ↑ |
| MS | 3693 ↓ | 0.025 ↓ | 0.010 ↓ | 0.024 ↓ | 0.055 ↓ |
| TS | 41 | 0.768 | 0.701 | 0.813 | 0.884 |
| Meta-Cal | 202 ↓ | 0.746 ↓ | 0.680 ↓ | 0.790 ↓ | 0.861 ↓ |
| PTS | 41 | 0.768 | 0.701 | 0.813 | 0.884 |
| KGEC | 41 | 0.768 | 0.701 | 0.813 | 0.884 |
| FB15K-237 | | | | | |
| Uncal | 174 | 0.309 | 0.222 | 0.337 | 0.484 |
| PS | 174 | 0.309 | 0.222 | 0.337 | 0.484 |
| HB | 2695 ↓ | 0.256 ↓ | 0.184 ↓ | 0.286 ↓ | 0.401 ↓ |
| IR | 2156 ↓ | 0.280 ↓ | 0.205 ↑ | 0.311 ↓ | 0.427 ↓ |
| BBQ | 1562 ↓ | 0.235 ↓ | 0.163 ↓ | 0.259 ↓ | 0.378 ↓ |
| VS | 172 ↑ | 0.305 ↓ | 0.216 ↓ | 0.333 ↓ | 0.484 |
| MS | 3704 ↓ | 0.033 ↓ | 0.014 ↓ | 0.032 ↓ | 0.070 ↓ |
| TS | 174 | 0.309 | 0.222 | 0.337 | 0.484 |
| Meta-Cal | 259 ↓ | 0.300 ↓ | 0.213 ↓ | 0.327 ↓ | 0.474 ↓ |
| PTS | 5659 ↓ | 0.222 ↓ | 0.222 | 0.222 ↓ | 0.223 ↓ |
| KGEC | 174 | 0.309 | 0.222 | 0.337 | 0.484 |

model, as shown in Figure 3 and Figure 4. These examples highlight how calibrated probabilities offer more interpretable and informative confidence scores compared to raw, uncalibrated scores.

Case 1: (Greece, _member_of_domain_region, ?) The ground-truth answer for this query is *sibyl*, which is ranked third among the candidate entities based on the model’s raw scores. However, the uncalibrated scores do not reflect a meaningful confidence distribution, with the top-ranked entity *Greece* receiving a score of -0.1873 and the correct answer *sibyl* receiving -0.5992 , a difference that is difficult to interpret probabilistically.

After applying KGEC calibration, the corresponding probabilities become more interpretable:

- *Greece*: 0.0302

- *Holy See*: 0.0272

- *sibyl* (true answer): 0.0200

These calibrated probabilities clearly reflect the uncertainty inherent in the model’s prediction. Although the correct answer is not ranked first, its probability is close to that of the top candidates, suggesting it is still a plausible prediction. This shows that KGEC can better express confidence levels, especially in cases with closely competing candidates.

Case 2: (North_Atlantic_Treaty_Organization, _member_meronym, ?) In this case, the true answer is *Netherlands*, which is correctly ranked second. The raw score of the correct answer (1.6756) is only slightly lower than that of the top-ranked entity *North Atlantic Treaty Organization* (1.9763),

Table 10: Effect of different calibration methods on the performance of the RotatE model across various datasets.

| Method | MR | MRR | HITS@1 | HITS@3 | HITS@10 |
|------------------|---------|---------|---------|---------|---------|
| WN18 | | | | | |
| Uncal | 270 | 0.950 | 0.944 | 0.952 | 0.960 |
| PS | 270 | 0.950 | 0.944 | 0.952 | 0.960 |
| HB | 13910 ↓ | 0.279 ↓ | 0.263 ↓ | 0.294 ↓ | 0.299 ↓ |
| IR | 13962 ↓ | 0.297 ↓ | 0.286 ↓ | 0.308 ↓ | 0.313 ↓ |
| BBQ | 13801 ↓ | 0.271 ↓ | 0.253 ↓ | 0.286 ↓ | 0.297 ↓ |
| VS | 270 | 0.950 | 0.944 | 0.952 | 0.960 |
| MS | 16626 ↓ | 0.013 ↓ | 0.005 ↓ | 0.013 ↓ | 0.027 ↓ |
| TS | 270 | 0.950 | 0.944 | 0.952 | 0.960 |
| Meta-Cal | 1917 ↓ | 0.905 ↓ | 0.904 ↓ | 0.905 ↓ | 0.905 ↓ |
| PTS | 474 ↓ | 0.949 ↓ | 0.944 | 0.951 ↓ | 0.958 ↓ |
| KGEC | 270 | 0.950 | 0.944 | 0.952 | 0.960 |
| WN18RR | | | | | |
| Uncal | 3421 | 0.476 | 0.429 | 0.496 | 0.570 |
| PS | 3421 | 0.476 | 0.429 | 0.497 ↑ | 0.570 |
| HB | 18719 ↓ | 0.114 ↓ | 0.104 ↓ | 0.122 ↓ | 0.127 ↓ |
| IR | 18047 ↓ | 0.118 ↓ | 0.103 ↓ | 0.128 ↓ | 0.143 ↓ |
| BBQ | 18189 ↓ | 0.086 ↓ | 0.073 ↓ | 0.095 ↓ | 0.105 ↓ |
| VS | 3422 ↓ | 0.476 | 0.429 | 0.497 ↑ | 0.570 |
| MS | 18195 ↓ | 0.009 ↓ | 0.003 ↓ | 0.008 ↓ | 0.020 ↓ |
| TS | 3421 | 0.476 | 0.429 | 0.497 ↑ | 0.570 |
| Meta-Cal | 6168 ↓ | 0.448 ↓ | 0.409 ↓ | 0.464 ↓ | 0.523 ↓ |
| PTS | 3776 ↓ | 0.474 ↓ | 0.429 | 0.493 ↓ | 0.564 ↓ |
| KGEC | 3421 | 0.476 | 0.429 | 0.497 ↑ | 0.570 |
| FB15K | | | | | |
| Uncal | 41 | 0.791 | 0.739 | 0.825 | 0.881 |
| PS | 41 | 0.791 | 0.739 | 0.825 | 0.881 |
| HB | 1843 ↓ | 0.642 ↓ | 0.588 ↓ | 0.682 ↓ | 0.731 ↓ |
| IR | 961 ↓ | 0.696 ↓ | 0.635 ↓ | 0.741 ↓ | 0.799 ↓ |
| BBQ | 1027 ↓ | 0.662 ↓ | 0.599 ↓ | 0.709 ↓ | 0.768 ↓ |
| VS | 42 ↓ | 0.791 | 0.739 | 0.825 | 0.880 ↓ |
| MS | 3693 ↓ | 0.025 ↓ | 0.010 ↓ | 0.024 ↓ | 0.055 ↓ |
| TS | 41 | 0.791 | 0.739 | 0.825 | 0.881 |
| Meta-Cal | 457 ↓ | 0.750 ↓ | 0.700 ↓ | 0.783 ↓ | 0.835 ↓ |
| PTS | 1122 ↓ | 0.763 ↓ | 0.739 | 0.782 ↓ | 0.801 ↓ |
| KGEC | 41 | 0.791 | 0.739 | 0.825 | 0.881 |
| FB15K-237 | | | | | |
| Uncal | 178 | 0.336 | 0.239 | 0.374 | 0.530 |
| PS | 178 | 0.336 | 0.239 | 0.374 | 0.530 |
| HB | 3458 ↓ | 0.285 ↓ | 0.221 ↓ | 0.317 ↓ | 0.412 ↓ |
| IR | 2131 ↓ | 0.307 ↓ | 0.232 ↓ | 0.340 ↓ | 0.455 ↓ |
| BBQ | 2292 ↓ | 0.275 ↓ | 0.204 ↓ | 0.305 ↓ | 0.415 ↓ |
| VS | 179 ↓ | 0.336 | 0.239 | 0.374 | 0.530 |
| MS | 3704 ↓ | 0.033 ↓ | 0.014 ↓ | 0.032 ↓ | 0.070 ↓ |
| TS | 178 | 0.336 | 0.239 | 0.374 | 0.530 |
| Meta-Cal | 246 ↓ | 0.328 ↓ | 0.232 ↓ | 0.365 ↓ | 0.522 ↓ |
| PTS | 179 ↓ | 0.336 | 0.239 | 0.374 | 0.530 |
| KGEC | 178 | 0.336 | 0.239 | 0.374 | 0.530 |

| Query: ('North_Atlantic_Treaty_Organization', _member_meronym, ?) | | |
|---|---------------------|--------------------------|
| True answer: Netherlands | | |
| Ranked candidate entities | Uncalibrated scores | Calibrated probabilities |
| 'North_Atlantic_Treaty_Organization | 1.9763 | 0.3756 |
| Netherlands | 1.6756 | 0.2781 |
| European_Union | 0.9763 | 0.1382 |
| Benelux | 0.9763 | 0.1382 |
| Apeldoorn | -0.4998 | 0.0316 |
| Leiden | -0.5236 | 0.0308 |
| Frisian_Islands | -0.5844 | 0.0290 |
| Friesland | -0.6578 | 0.0270 |
| Netherlander | -0.6780 | 0.0264 |
| British_Commonwealth | -0.7083 | 0.0256 |

Figure 4: Case 2 from the WN18RR dataset using the TransE model.

Insights. These case studies demonstrate that:

- KGEC enhances the interpretability of model outputs by transforming unnormalized scores into well-calibrated probabilities.
- It allows more accurate reflection of confidence levels, particularly in ambiguous or competitive ranking situations.
- Even when the top-1 prediction is incorrect, KGEC highlights alternative candidates with meaningful confidence, which is valuable for applications such as knowledge graph reasoning, question answering, and downstream ensemble methods.

Overall, these cases exemplify the effectiveness of KGEC in improving the trustworthiness and usability of KGE models.

but the significance of this difference is unclear without proper calibration.

With KGEC, the calibrated probabilities provide a more informative picture:

- *North Atlantic Treaty Organization*: 0.3756
- *Netherlands* (true answer): 0.2781
- *European Union*: 0.1382

Here, although the true answer is not ranked first, its calibrated probability is still relatively high, reflecting the model's uncertainty and partially shared semantics among top candidates. This enables downstream applications to interpret and potentially leverage multiple candidates rather than over-committing to the top-1 prediction.

Table 11: Effect of each component in KGEC on the performance and efficiency of various KGE models across multiple datasets. For all the five metrics, the lower the better.

| <i>ECE</i> | <i>TransE</i> | | | | <i>ComplEx</i> | | | | <i>DistMult</i> | | | | <i>RotatE</i> | | | | <i>Average</i> |
|-------------------|---------------|---------------|--------------|------------------|----------------|---------------|--------------|------------------|-----------------|---------------|--------------|------------------|---------------|---------------|--------------|------------------|----------------|
| | <i>WN18</i> | <i>WN18RR</i> | <i>FB15K</i> | <i>FB15K-237</i> | <i>WN18</i> | <i>WN18RR</i> | <i>FB15K</i> | <i>FB15K-237</i> | <i>WN18</i> | <i>WN18RR</i> | <i>FB15K</i> | <i>FB15K-237</i> | <i>WN18</i> | <i>WN18RR</i> | <i>FB15K</i> | <i>FB15K-237</i> | |
| KGEC-loss-MBS-JSS | 0.642 | 0.195 | 0.637 | 0.213 | 0.852 | 0.423 | 0.691 | 0.228 | 0.528 | 0.389 | 0.689 | 0.220 | 0.805 | 0.383 | 0.671 | 0.222 | 0.487 |
| KGEC-loss-MBS | 0.634 | 0.196 | 0.637 | 0.213 | 0.852 | 0.423 | 0.691 | 0.228 | 0.528 | 0.389 | 0.688 | 0.220 | 0.821 | 0.383 | 0.672 | 0.222 | 0.487 |
| KGEC-loss | 0.611 | 0.196 | 0.408 | 0.199 | 0.824 | 0.377 | 0.689 | 0.161 | 0.501 | 0.388 | 0.683 | 0.165 | 0.813 | 0.327 | 0.642 | 0.215 | 0.450 |
| KGEC | 0.171 | 0.280 | 0.459 | 0.150 | 0.833 | 0.418 | 0.678 | 0.189 | 0.446 | 0.383 | 0.683 | 0.178 | 0.467 | 0.307 | 0.466 | 0.094 | 0.388 |

| <i>ACE</i> | <i>TransE</i> | | | | <i>ComplEx</i> | | | | <i>DistMult</i> | | | | <i>RotatE</i> | | | | <i>Average</i> |
|-------------------|---------------|---------------|--------------|------------------|----------------|---------------|--------------|------------------|-----------------|---------------|--------------|------------------|---------------|---------------|--------------|------------------|----------------|
| | <i>WN18</i> | <i>WN18RR</i> | <i>FB15K</i> | <i>FB15K-237</i> | <i>WN18</i> | <i>WN18RR</i> | <i>FB15K</i> | <i>FB15K-237</i> | <i>WN18</i> | <i>WN18RR</i> | <i>FB15K</i> | <i>FB15K-237</i> | <i>WN18</i> | <i>WN18RR</i> | <i>FB15K</i> | <i>FB15K-237</i> | |
| KGEC-loss-MBS-JSS | 0.517 | 0.285 | 0.636 | 0.168 | 0.852 | 0.423 | 0.691 | 0.227 | 0.527 | 0.389 | 0.688 | 0.220 | 0.405 | 0.383 | 0.636 | 0.220 | 0.454 |
| KGEC-loss-MBS | 0.516 | 0.285 | 0.630 | 0.168 | 0.852 | 0.423 | 0.690 | 0.227 | 0.527 | 0.389 | 0.688 | 0.220 | 0.402 | 0.383 | 0.636 | 0.220 | 0.454 |
| KGEC-loss | 0.510 | 0.283 | 7.651 | 0.943 | 0.823 | 0.350 | 0.670 | 0.161 | 0.501 | 0.388 | 0.666 | 0.163 | 0.401 | 0.278 | 3.092 | 0.308 | 1.074 |
| KGEC | 0.131 | 0.277 | 0.293 | 0.082 | 0.833 | 0.418 | 0.465 | 0.207 | 0.457 | 0.383 | 0.516 | 0.199 | 0.467 | 0.306 | 0.466 | 0.063 | 0.348 |

| <i>NLL</i> | <i>TransE</i> | | | | <i>ComplEx</i> | | | | <i>DistMult</i> | | | | <i>RotatE</i> | | | | <i>Average</i> |
|-------------------|---------------|---------------|--------------|------------------|----------------|---------------|--------------|------------------|-----------------|---------------|--------------|------------------|---------------|---------------|--------------|------------------|----------------|
| | <i>WN18</i> | <i>WN18RR</i> | <i>FB15K</i> | <i>FB15K-237</i> | <i>WN18</i> | <i>WN18RR</i> | <i>FB15K</i> | <i>FB15K-237</i> | <i>WN18</i> | <i>WN18RR</i> | <i>FB15K</i> | <i>FB15K-237</i> | <i>WN18</i> | <i>WN18RR</i> | <i>FB15K</i> | <i>FB15K-237</i> | |
| KGEC-loss-MBS-JSS | 2.827 | 6.544 | 3.270 | 5.177 | 6.830 | 7.777 | 5.329 | 7.294 | 7.384 | 7.820 | 5.294 | 7.485 | 1.313 | 6.107 | 3.465 | 5.531 | 5.590 |
| KGEC-loss-MBS | 2.834 | 6.544 | 3.310 | 5.189 | 6.831 | 7.778 | 5.311 | 7.300 | 7.384 | 7.812 | 5.265 | 7.479 | 1.304 | 6.107 | 3.470 | 5.521 | 5.590 |
| KGEC-loss | 2.834 | 6.330 | 0.687 | 4.093 | 4.856 | 7.636 | 6.732 | 3.811 | 5.407 | 7.772 | 6.444 | 3.950 | 1.309 | 6.327 | 5.014 | 6.156 | 4.960 |
| KGEC | 2.462 | 5.965 | 2.536 | 2.889 | 4.350 | 6.965 | 1.357 | 2.911 | 2.843 | 7.119 | 1.319 | 3.106 | 1.036 | 4.698 | 2.033 | 2.743 | 3.396 |

| <i>Training Time / s</i> | <i>TransE</i> | | | | <i>ComplEx</i> | | | | <i>DistMult</i> | | | | <i>RotatE</i> | | | | <i>Average</i> |
|--------------------------|---------------|---------------|--------------|------------------|----------------|---------------|--------------|------------------|-----------------|---------------|--------------|------------------|---------------|---------------|--------------|------------------|----------------|
| | <i>WN18</i> | <i>WN18RR</i> | <i>FB15K</i> | <i>FB15K-237</i> | <i>WN18</i> | <i>WN18RR</i> | <i>FB15K</i> | <i>FB15K-237</i> | <i>WN18</i> | <i>WN18RR</i> | <i>FB15K</i> | <i>FB15K-237</i> | <i>WN18</i> | <i>WN18RR</i> | <i>FB15K</i> | <i>FB15K-237</i> | |
| KGEC-loss-MBS-JSS | 39.769 | 24.194 | 139.544 | 54.700 | 40.996 | 23.856 | 148.151 | 50.186 | 39.602 | 24.557 | 147.145 | 52.021 | 39.659 | 24.270 | 153.269 | 52.023 | 65.871 |
| KGEC-loss-MBS | 2.894 | 1.638 | 11.442 | 3.598 | 2.714 | 1.611 | 10.166 | 3.546 | 2.661 | 1.645 | 10.147 | 3.603 | 2.825 | 1.608 | 10.760 | 3.695 | 4.659 |
| KGEC-loss | 2.785 | 1.676 | 10.305 | 3.598 | 2.915 | 1.650 | 10.246 | 3.597 | 2.660 | 1.644 | 10.490 | 3.527 | 2.671 | 1.605 | 10.747 | 3.578 | 4.606 |
| KGEC | 2.727 | 1.776 | 10.873 | 3.602 | 2.698 | 1.727 | 10.560 | 3.624 | 2.741 | 1.696 | 10.645 | 3.705 | 2.662 | 1.658 | 10.758 | 4.003 | 4.716 |

| <i>Memory Usage / MB</i> | <i>TransE</i> | | | | <i>ComplEx</i> | | | | <i>DistMult</i> | | | | <i>RotatE</i> | | | | <i>Average</i> |
|--------------------------|---------------|---------------|--------------|------------------|----------------|---------------|--------------|------------------|-----------------|---------------|--------------|------------------|---------------|---------------|--------------|------------------|----------------|
| | <i>WN18</i> | <i>WN18RR</i> | <i>FB15K</i> | <i>FB15K-237</i> | <i>WN18</i> | <i>WN18RR</i> | <i>FB15K</i> | <i>FB15K-237</i> | <i>WN18</i> | <i>WN18RR</i> | <i>FB15K</i> | <i>FB15K-237</i> | <i>WN18</i> | <i>WN18RR</i> | <i>FB15K</i> | <i>FB15K-237</i> | |
| KGEC-loss-MBS-JSS | 161.801 | 126.141 | 58.465 | 50.965 | 170.859 | 111.168 | 41.953 | 65.574 | 174.496 | 124.086 | 56.414 | 56.473 | 160.766 | 94.270 | 45.000 | 63.301 | 97.608 |
| KGEC-loss-MBS | 29.027 | 27.121 | 6.871 | 17.969 | 31.258 | 26.676 | 7.535 | 10.391 | 25.426 | 27.184 | 8.750 | 14.277 | 32.906 | 30.742 | 6.422 | 17.961 | 20.032 |
| KGEC-loss | 29.414 | 27.145 | 6.898 | 18.016 | 25.645 | 26.879 | 8.145 | 10.375 | 32.254 | 26.613 | 8.695 | 14.320 | 32.754 | 30.965 | 10.172 | 17.316 | 20.350 |
| KGEC | 30.484 | 28.289 | 7.570 | 15.273 | 26.652 | 32.176 | 9.535 | 15.285 | 34.316 | 32.047 | 10.531 | 13.492 | 34.320 | 32.191 | 7.551 | 16.930 | 21.665 |

Table 12: Effect of different number of bins in KGEC on the performance of various KGE models across multiple datasets. For all the three metrics, the lower the better.

| ECE | TransE | | | | Complex | | | | DistMult | | | | RotatE | | | | Average |
|--------|--------|--------|-------|-----------|---------|--------|-------|-----------|----------|--------|-------|-----------|--------|--------|-------|-----------|---------|
| | WN18 | WN18RR | FB15K | FB15K-237 | WN18 | WN18RR | FB15K | FB15K-237 | WN18 | WN18RR | FB15K | FB15K-237 | WN18 | WN18RR | FB15K | FB15K-237 | |
| Bin=1 | 0.702 | 0.196 | 0.586 | 0.198 | 0.851 | 0.422 | 0.642 | 0.227 | 0.527 | 0.389 | 0.687 | 0.221 | 0.904 | 0.382 | 0.663 | 0.222 | 0.489 |
| Bin=2 | 0.305 | 0.316 | 0.581 | 0.184 | 0.850 | 0.422 | 0.677 | 0.190 | 0.521 | 0.387 | 0.683 | 0.219 | 0.476 | 0.305 | 0.671 | 0.105 | 0.431 |
| Bin=3 | 0.214 | 0.238 | 0.498 | 0.183 | 0.848 | 0.422 | 0.677 | 0.190 | 0.515 | 0.385 | 0.683 | 0.180 | 0.467 | 0.293 | 0.653 | 0.101 | 0.409 |
| Bin=4 | 0.245 | 0.249 | 0.491 | 0.180 | 0.848 | 0.421 | 0.677 | 0.190 | 0.447 | 0.385 | 0.682 | 0.179 | 0.486 | 0.286 | 0.646 | 0.098 | 0.407 |
| Bin=5 | 0.235 | 0.262 | 0.479 | 0.182 | 0.848 | 0.420 | 0.677 | 0.189 | 0.447 | 0.385 | 0.682 | 0.179 | 0.470 | 0.297 | 0.622 | 0.102 | 0.405 |
| Bin=6 | 0.211 | 0.260 | 0.514 | 0.170 | 0.848 | 0.419 | 0.677 | 0.189 | 0.447 | 0.384 | 0.682 | 0.179 | 0.487 | 0.290 | 0.584 | 0.112 | 0.403 |
| Bin=7 | 0.159 | 0.273 | 0.457 | 0.147 | 0.848 | 0.418 | 0.678 | 0.189 | 0.447 | 0.384 | 0.682 | 0.179 | 0.451 | 0.304 | 0.593 | 0.104 | 0.394 |
| Bin=8 | 0.194 | 0.269 | 0.460 | 0.161 | 0.848 | 0.418 | 0.678 | 0.189 | 0.446 | 0.384 | 0.682 | 0.179 | 0.464 | 0.307 | 0.529 | 0.126 | 0.396 |
| Bin=9 | 0.181 | 0.276 | 0.444 | 0.160 | 0.841 | 0.418 | 0.678 | 0.189 | 0.446 | 0.384 | 0.683 | 0.178 | 0.464 | 0.305 | 0.498 | 0.157 | 0.394 |
| Bin=10 | 0.171 | 0.280 | 0.459 | 0.150 | 0.833 | 0.418 | 0.678 | 0.189 | 0.446 | 0.383 | 0.683 | 0.178 | 0.467 | 0.307 | 0.466 | 0.094 | 0.388 |
| Bin=11 | 0.164 | 0.283 | 0.416 | 0.137 | 0.833 | 0.418 | 0.678 | 0.189 | 0.446 | 0.383 | 0.683 | 0.178 | 0.476 | 0.316 | 0.491 | 0.093 | 0.387 |
| Bin=12 | 0.163 | 0.281 | 0.388 | 0.162 | 0.833 | 0.418 | 0.678 | 0.189 | 0.446 | 0.383 | 0.683 | 0.178 | 0.475 | 0.316 | 0.475 | 0.100 | 0.386 |
| Bin=13 | 0.148 | 0.287 | 0.370 | 0.123 | 0.835 | 0.418 | 0.678 | 0.189 | 0.446 | 0.383 | 0.683 | 0.178 | 0.471 | 0.317 | 0.459 | 0.086 | 0.379 |
| Bin=14 | 0.125 | 0.293 | 0.376 | 0.140 | 0.835 | 0.417 | 0.677 | 0.189 | 0.446 | 0.382 | 0.683 | 0.178 | 0.472 | 0.319 | 0.458 | 0.116 | 0.381 |
| Bin=15 | 0.102 | 0.294 | 0.336 | 0.129 | 0.824 | 0.417 | 0.678 | 0.189 | 0.446 | 0.381 | 0.682 | 0.178 | 0.475 | 0.318 | 0.461 | 0.076 | 0.374 |
| Bin=16 | 0.154 | 0.296 | 0.349 | 0.061 | 0.769 | 0.416 | 0.677 | 0.189 | 0.446 | 0.379 | 0.682 | 0.178 | 0.472 | 0.319 | 0.494 | 0.087 | 0.373 |
| Bin=17 | 0.120 | 0.296 | 0.313 | 0.064 | 0.764 | 0.415 | 0.585 | 0.189 | 0.446 | 0.377 | 0.682 | 0.178 | 0.478 | 0.324 | 0.490 | 0.091 | 0.363 |
| Bin=18 | 0.115 | 0.293 | 0.256 | 0.085 | 0.749 | 0.415 | 0.589 | 0.189 | 0.446 | 0.377 | 0.640 | 0.178 | 0.472 | 0.325 | 0.489 | 0.134 | 0.360 |
| Bin=19 | 0.113 | 0.293 | 0.256 | 0.084 | 0.749 | 0.415 | 0.579 | 0.189 | 0.446 | 0.377 | 0.603 | 0.178 | 0.482 | 0.326 | 0.488 | 0.062 | 0.352 |
| Bin=20 | 0.135 | 0.298 | 0.261 | 0.073 | 0.753 | 0.416 | 0.580 | 0.189 | 0.445 | 0.376 | 0.577 | 0.178 | 0.478 | 0.319 | 0.493 | 0.046 | 0.351 |

| ACE | TransE | | | | Complex | | | | DistMult | | | | RotatE | | | | Average |
|--------|--------|--------|-------|-----------|---------|--------|-------|-----------|----------|--------|-------|-----------|--------|--------|-------|-----------|---------|
| | WN18 | WN18RR | FB15K | FB15K-237 | WN18 | WN18RR | FB15K | FB15K-237 | WN18 | WN18RR | FB15K | FB15K-237 | WN18 | WN18RR | FB15K | FB15K-237 | |
| Bin=1 | 0.598 | 0.285 | 0.565 | 0.158 | 0.851 | 0.422 | 0.633 | 0.227 | 0.527 | 0.389 | 0.686 | 0.221 | 0.385 | 0.382 | 0.602 | 0.220 | 0.447 |
| Bin=2 | 0.318 | 0.323 | 0.406 | 0.128 | 0.849 | 0.422 | 0.494 | 0.217 | 0.519 | 0.387 | 0.538 | 0.217 | 0.476 | 0.242 | 0.495 | 0.093 | 0.383 |
| Bin=3 | 0.232 | 0.243 | 0.378 | 0.104 | 0.848 | 0.422 | 0.491 | 0.217 | 0.511 | 0.385 | 0.533 | 0.217 | 0.467 | 0.226 | 0.471 | 0.076 | 0.364 |
| Bin=4 | 0.171 | 0.253 | 0.328 | 0.097 | 0.848 | 0.421 | 0.488 | 0.213 | 0.460 | 0.385 | 0.530 | 0.213 | 0.449 | 0.281 | 0.450 | 0.082 | 0.354 |
| Bin=5 | 0.155 | 0.264 | 0.307 | 0.099 | 0.848 | 0.420 | 0.484 | 0.211 | 0.460 | 0.385 | 0.529 | 0.210 | 0.458 | 0.297 | 0.441 | 0.069 | 0.352 |
| Bin=6 | 0.125 | 0.262 | 0.261 | 0.083 | 0.848 | 0.419 | 0.481 | 0.210 | 0.460 | 0.384 | 0.527 | 0.204 | 0.457 | 0.290 | 0.454 | 0.070 | 0.346 |
| Bin=7 | 0.135 | 0.271 | 0.277 | 0.061 | 0.848 | 0.418 | 0.478 | 0.209 | 0.460 | 0.384 | 0.526 | 0.204 | 0.451 | 0.304 | 0.419 | 0.067 | 0.345 |
| Bin=8 | 0.129 | 0.267 | 0.264 | 0.080 | 0.848 | 0.418 | 0.475 | 0.208 | 0.457 | 0.384 | 0.522 | 0.203 | 0.464 | 0.307 | 0.456 | 0.072 | 0.347 |
| Bin=9 | 0.142 | 0.274 | 0.270 | 0.085 | 0.841 | 0.418 | 0.471 | 0.208 | 0.457 | 0.384 | 0.521 | 0.200 | 0.463 | 0.305 | 0.454 | 0.099 | 0.349 |
| Bin=10 | 0.131 | 0.277 | 0.293 | 0.082 | 0.833 | 0.418 | 0.465 | 0.207 | 0.457 | 0.383 | 0.516 | 0.199 | 0.467 | 0.306 | 0.466 | 0.063 | 0.348 |
| Bin=11 | 0.111 | 0.280 | 0.278 | 0.076 | 0.833 | 0.418 | 0.460 | 0.207 | 0.457 | 0.383 | 0.513 | 0.199 | 0.461 | 0.316 | 0.491 | 0.061 | 0.347 |
| Bin=12 | 0.107 | 0.278 | 0.259 | 0.100 | 0.833 | 0.418 | 0.456 | 0.207 | 0.457 | 0.383 | 0.508 | 0.199 | 0.475 | 0.316 | 0.475 | 0.061 | 0.346 |
| Bin=13 | 0.128 | 0.284 | 0.240 | 0.077 | 0.834 | 0.418 | 0.450 | 0.206 | 0.457 | 0.383 | 0.503 | 0.197 | 0.471 | 0.316 | 0.459 | 0.059 | 0.343 |
| Bin=14 | 0.113 | 0.291 | 0.238 | 0.088 | 0.834 | 0.417 | 0.446 | 0.205 | 0.455 | 0.382 | 0.497 | 0.196 | 0.471 | 0.319 | 0.458 | 0.062 | 0.342 |
| Bin=15 | 0.107 | 0.292 | 0.239 | 0.086 | 0.823 | 0.417 | 0.441 | 0.204 | 0.455 | 0.381 | 0.492 | 0.195 | 0.475 | 0.318 | 0.461 | 0.057 | 0.340 |
| Bin=16 | 0.111 | 0.294 | 0.234 | 0.063 | 0.767 | 0.416 | 0.436 | 0.204 | 0.455 | 0.379 | 0.486 | 0.194 | 0.472 | 0.319 | 0.494 | 0.053 | 0.336 |
| Bin=17 | 0.100 | 0.296 | 0.237 | 0.064 | 0.762 | 0.415 | 0.550 | 0.204 | 0.453 | 0.377 | 0.481 | 0.193 | 0.478 | 0.324 | 0.490 | 0.053 | 0.342 |
| Bin=18 | 0.119 | 0.293 | 0.248 | 0.083 | 0.746 | 0.415 | 0.576 | 0.204 | 0.453 | 0.377 | 0.466 | 0.192 | 0.471 | 0.325 | 0.489 | 0.075 | 0.346 |
| Bin=19 | 0.115 | 0.293 | 0.247 | 0.090 | 0.746 | 0.415 | 0.534 | 0.203 | 0.453 | 0.377 | 0.482 | 0.192 | 0.482 | 0.326 | 0.488 | 0.046 | 0.343 |
| Bin=20 | 0.107 | 0.298 | 0.249 | 0.073 | 0.750 | 0.416 | 0.557 | 0.203 | 0.450 | 0.376 | 0.553 | 0.192 | 0.478 | 0.319 | 0.493 | 0.048 | 0.348 |

| NLL | TransE | | | | Complex | | | | DistMult | | | | RotatE | | | | Average |
|--------|--------|--------|-------|-----------|---------|--------|-------|-----------|----------|--------|-------|-----------|--------|--------|-------|-----------|---------|
| | WN18 | WN18RR | FB15K | FB15K-237 | WN18 | WN18RR | FB15K | FB15K-237 | WN18 | WN18RR | FB15K | FB15K-237 | WN18 | WN18RR | FB15K | FB15K-237 | |
| Bin=1 | 2.544 | 6.543 | 3.910 | 4.774 | 6.524 | 7.496 | 3.589 | 7.208 | 6.944 | 7.947 | 5.152 | 8.395 | 1.165 | 6.078 | 3.184 | 5.515 | 5.436 |
| Bin=2 | 2.865 | 6.212 | 3.076 | 3.365 | 5.963 | 7.513 | 1.350 | 2.908 | 5.477 | 7.578 | 1.314 | 6.650 | 1.281 | 4.606 | 1.989 | 3.056 | 4.075 |
| Bin=3 | 2.712 | 6.265 | 2.986 | 3.290 | 5.633 | 7.513 | 1.350 | 2.908 | 4.913 | 7.338 | 1.315 | 3.101 | 1.184 | 4.472 | 2.042 | 2.774 | 3.737 |
| Bin=4 | 2.605 | 6.185 | 2.845 | 3.191 | 5.633 | 7.299 | 1.351 | 2.909 | 2.843 | 7.338 | 1.315 | 3.101 | 1.100 | 4.745 | 1.974 | 2.911 | 3.584 |
| Bin=5 | 2.537 | 6.109 | 2.766 | 3.061 | 5.633 | 7.202 | 1.351 | 2.909 | 2.843 | 7.338 | 1.315 | 3.102 | 1.088 | 4.821 | 2.011 | 2.713 | 3.550 |
| Bin=6 | 2.523 | 6.085 | 2.642 | 3.062 | 5.633 | 7.123 | 1.352 | 2.909 | 2.843 | 7.200 | 1.316 | 3.104 | 1.062 | 4.716 | 2.083 | 2.643 | 3.518 |
| Bin=7 | 2.515 | 6.023 | 2.641 | 3.112 | 5.633 | 7.009 | 1.352 | 2.910 | 2.843 | 7.200 | 1.316 | 3.104 | 1.038 | 4.787 | 1.939 | 2.672 | 3.506 |
| Bin=8 | 2.499 | 6.024 | 2.607 | 2.956 | 5.656 | 7.001 | 1.353 | 2.910 | 2.844 | 7.200 | 1.317 | 3.104 | 1.051 | 4.772 | 2.039 | 2.580 | 3.495 |
| Bin=9 | 2.493 | 5.987 | 2.602 | 2.895 | 4.835 | 6.965 | 1.355 | 2.910 | 2.843 | 7.200 | 1.317 | 3.105 | 1.035 | 4.711 | 2.011 | 2.473 | 3.421 |
| Bin=10 | 2.462 | 5.965 | 2.536 | 2.889 | 4.350 | 6.965 | 1.357 | 2.911 | 2.843 | 7.119 | 1.319 | 3.106 | 1.036 | 4.698 | 2.033 | 2.743 | 3.396 |
| Bin=11 | 2.466 | 5.944 | 2.532 | 2.898 | 4.350 | 6.965 | 1.358 | 2.911 | 2.843 | 7.119 | 1.319 | 3.106 | 1.013 | 4.754 | 2.123 | 2.743 | 3.403 |
| Bin=12 | 2.448 | 5.943 | 2.529 | 2.798 | 4.350 | 6.929 | 1.359 | 2.911 | 2.843 | 7.114 | 1.321 | 3.106 | 1.043 | 4.731 | 2.037 | 2.666 | 3.383 |
| Bin=13 | 2.447 | 5.919 | 2.486 | 2.871 | 4.415 | 6.933 | 1.360 | 2.911 | 2.843 | 7.114 | 1.323 | 3.107 | 1.022 | 4.714 | 1.959 | 2.772 | 3.387 |
| Bin=14 | 2.437 | 5.889 | 2.482 | 2.809 | 4.415 | 6.867 | 1.363 | 2.912 | 2.845 | 7.027 | 1.326 | 3.108 | 1.017 | 4.714 | 1.941 | 2.593 | 3.359 |
| Bin=15 | 2.438 | 5.880 | 2.498 | 2.803 | 3.987 | 6.867 | 1.363 | 2.912 | 2.845 | 6.935 | 1.329 | 3.108 | 1.024 | 4.689 | 1.942 | 2.813 | 3.340 |
| Bin=16 | 2.449 | 5.870 | 2.463 | 2.883 | 2.931 | 6.773 | 1.366 | 2.912 | 2.845 | 6.813 | 1.331 | 3.109 | 1.014 | 4.684 | 2.060 | 2.669 | 3.261 |
| Bin=17 | 2.434 | 5.859 | 2.487 | 2.855 | 2.873 | 6.726 | 2.678 | 2.913 | 2.846 | 6.722 | 1.333 | 3.109 | 1.023 | 4.722 | 2.030 | 2.638 | 3.328 |
| Bin=18 | 2.449 | 5.865 | 2.513 | 2.779 | 2.711 | 6.724 | 2.860 | 2.913 | 2.84 | | | | | | | | |

Table 13: Effect of different initial temperature parameters in KGEC on the performance of various KGE models across multiple datasets. For all the three metrics, the lower the better.

| ECE | TransE | | | | ComplEx | | | | DistMult | | | | RotatE | | | | Average |
|----------|--------|--------|-------|-----------|---------|--------|-------|-----------|----------|--------|-------|-----------|--------|--------|-------|-----------|---------|
| | WN18 | WN18RR | FB15K | FB15K-237 | WN18 | WN18RR | FB15K | FB15K-237 | WN18 | WN18RR | FB15K | FB15K-237 | WN18 | WN18RR | FB15K | FB15K-237 | |
| init=0 | 0.382 | 0.582 | 0.405 | 0.213 | 0.699 | 0.374 | 0.677 | 0.190 | 0.447 | 0.349 | 0.683 | 0.180 | 0.118 | 0.322 | 0.612 | 0.237 | 0.404 |
| init=0.1 | 0.382 | 0.582 | 0.312 | 0.213 | 0.699 | 0.374 | 0.677 | 0.190 | 0.447 | 0.349 | 0.683 | 0.180 | 0.118 | 0.389 | 0.670 | 0.236 | 0.406 |
| init=0.2 | 0.337 | 0.014 | 0.626 | 0.221 | 0.699 | 0.374 | 0.678 | 0.189 | 0.447 | 0.349 | 0.683 | 0.179 | 0.603 | 0.420 | 0.719 | 0.239 | 0.424 |
| init=0.3 | 0.696 | 0.013 | 0.626 | 0.221 | 0.699 | 0.374 | 0.678 | 0.189 | 0.447 | 0.349 | 0.683 | 0.179 | 0.939 | 0.428 | 0.719 | 0.239 | 0.467 |
| init=0.4 | 0.705 | 0.014 | 0.627 | 0.221 | 0.699 | 0.374 | 0.678 | 0.189 | 0.447 | 0.349 | 0.683 | 0.178 | 0.944 | 0.426 | 0.729 | 0.239 | 0.469 |
| init=0.5 | 0.706 | 0.014 | 0.645 | 0.221 | 0.699 | 0.279 | 0.678 | 0.189 | 0.447 | 0.222 | 0.683 | 0.178 | 0.944 | 0.397 | 0.709 | 0.239 | 0.453 |
| init=0.6 | 0.706 | 0.268 | 0.624 | 0.233 | 0.699 | 0.348 | 0.678 | 0.189 | 0.447 | 0.336 | 0.683 | 0.178 | 0.944 | 0.320 | 0.668 | 0.239 | 0.472 |
| init=0.7 | 0.706 | 0.390 | 0.566 | 0.233 | 0.699 | 0.384 | 0.678 | 0.189 | 0.447 | 0.356 | 0.683 | 0.178 | 0.907 | 0.244 | 0.597 | 0.239 | 0.468 |
| init=0.8 | 0.706 | 0.424 | 0.520 | 0.226 | 0.793 | 0.404 | 0.678 | 0.189 | 0.446 | 0.370 | 0.683 | 0.178 | 0.355 | 0.215 | 0.530 | 0.173 | 0.431 |
| init=0.9 | 0.444 | 0.342 | 0.496 | 0.200 | 0.823 | 0.412 | 0.678 | 0.189 | 0.446 | 0.376 | 0.683 | 0.178 | 0.402 | 0.273 | 0.492 | 0.124 | 0.410 |
| init=1.0 | 0.171 | 0.280 | 0.459 | 0.150 | 0.833 | 0.418 | 0.678 | 0.189 | 0.446 | 0.383 | 0.683 | 0.178 | 0.467 | 0.307 | 0.466 | 0.094 | 0.388 |
| init=1.1 | 0.199 | 0.232 | 0.419 | 0.109 | 0.848 | 0.420 | 0.678 | 0.189 | 0.446 | 0.386 | 0.683 | 0.178 | 0.547 | 0.331 | 0.495 | 0.098 | 0.391 |
| init=1.2 | 0.278 | 0.195 | 0.365 | 0.073 | 0.849 | 0.422 | 0.606 | 0.189 | 0.485 | 0.388 | 0.683 | 0.178 | 0.608 | 0.350 | 0.528 | 0.101 | 0.394 |
| init=1.3 | 0.340 | 0.165 | 0.335 | 0.051 | 0.850 | 0.423 | 0.592 | 0.189 | 0.513 | 0.388 | 0.683 | 0.178 | 0.656 | 0.362 | 0.551 | 0.106 | 0.399 |
| init=1.4 | 0.390 | 0.141 | 0.360 | 0.064 | 0.851 | 0.424 | 0.618 | 0.189 | 0.519 | 0.390 | 0.683 | 0.178 | 0.696 | 0.373 | 0.568 | 0.108 | 0.409 |
| init=1.5 | 0.430 | 0.122 | 0.388 | 0.082 | 0.852 | 0.425 | 0.599 | 0.190 | 0.524 | 0.390 | 0.602 | 0.178 | 0.727 | 0.382 | 0.581 | 0.133 | 0.413 |
| init=1.6 | 0.463 | 0.105 | 0.411 | 0.097 | 0.852 | 0.425 | 0.625 | 0.209 | 0.525 | 0.391 | 0.597 | 0.178 | 0.752 | 0.390 | 0.594 | 0.128 | 0.421 |
| init=1.7 | 0.491 | 0.090 | 0.429 | 0.110 | 0.852 | 0.425 | 0.611 | 0.213 | 0.526 | 0.391 | 0.609 | 0.193 | 0.773 | 0.395 | 0.609 | 0.150 | 0.429 |
| init=1.8 | 0.515 | 0.079 | 0.447 | 0.121 | 0.853 | 0.426 | 0.607 | 0.223 | 0.527 | 0.392 | 0.611 | 0.186 | 0.791 | 0.400 | 0.622 | 0.162 | 0.435 |
| init=1.9 | 0.534 | 0.069 | 0.462 | 0.133 | 0.853 | 0.426 | 0.616 | 0.223 | 0.527 | 0.392 | 0.614 | 0.198 | 0.807 | 0.404 | 0.631 | 0.167 | 0.441 |
| init=2.0 | 0.550 | 0.061 | 0.475 | 0.141 | 0.853 | 0.426 | 0.644 | 0.225 | 0.528 | 0.392 | 0.613 | 0.209 | 0.820 | 0.407 | 0.638 | 0.172 | 0.447 |

| ACE | TransE | | | | ComplEx | | | | DistMult | | | | RotatE | | | | Average |
|----------|--------|--------|--------|-----------|---------|--------|-------|-----------|----------|--------|-------|-----------|--------|--------|-------|-----------|---------|
| | WN18 | WN18RR | FB15K | FB15K-237 | WN18 | WN18RR | FB15K | FB15K-237 | WN18 | WN18RR | FB15K | FB15K-237 | WN18 | WN18RR | FB15K | FB15K-237 | |
| init=0 | 55.708 | 27.896 | 26.189 | 4.896 | 0.679 | 0.163 | 0.515 | 0.226 | 0.471 | 0.240 | 0.547 | 0.228 | 50.620 | 3.966 | 4.828 | 1.306 | 11.155 |
| init=0.1 | 37.388 | 18.451 | 12.026 | 4.896 | 0.679 | 0.163 | 0.515 | 0.226 | 0.471 | 0.240 | 0.547 | 0.228 | 27.979 | 3.158 | 4.275 | 1.278 | 7.032 |
| init=0.2 | 8.518 | 4.825 | 2.672 | 1.805 | 0.688 | 0.160 | 0.467 | 0.210 | 0.458 | 0.238 | 0.517 | 0.201 | 8.266 | 1.911 | 2.159 | 0.995 | 2.131 |
| init=0.3 | 4.237 | 2.449 | 2.671 | 1.805 | 0.688 | 0.160 | 0.466 | 0.208 | 0.458 | 0.238 | 0.517 | 0.200 | 3.453 | 1.006 | 2.154 | 0.995 | 1.357 |
| init=0.4 | 2.585 | 1.508 | 2.646 | 1.814 | 0.688 | 0.160 | 0.465 | 0.208 | 0.457 | 0.238 | 0.516 | 0.200 | 1.404 | 0.483 | 0.288 | 0.995 | 0.916 |
| init=0.5 | 1.535 | 0.994 | 0.311 | 1.795 | 0.688 | 0.265 | 0.465 | 0.207 | 0.457 | 0.208 | 0.516 | 0.200 | 0.726 | 0.195 | 0.298 | 0.995 | 0.616 |
| init=0.6 | 0.947 | 0.721 | 0.249 | 0.392 | 0.688 | 0.347 | 0.465 | 0.207 | 0.457 | 0.335 | 0.516 | 0.200 | 0.314 | 0.119 | 0.327 | 0.994 | 0.455 |
| init=0.7 | 0.573 | 0.542 | 0.242 | 0.290 | 0.689 | 0.384 | 0.465 | 0.207 | 0.457 | 0.355 | 0.516 | 0.199 | 0.105 | 0.152 | 0.362 | 0.994 | 0.408 |
| init=0.8 | 0.307 | 0.422 | 0.257 | 0.209 | 0.792 | 0.404 | 0.465 | 0.207 | 0.457 | 0.369 | 0.516 | 0.199 | 0.230 | 0.213 | 0.402 | 0.113 | 0.348 |
| init=0.9 | 0.144 | 0.339 | 0.275 | 0.141 | 0.822 | 0.412 | 0.465 | 0.207 | 0.457 | 0.376 | 0.516 | 0.199 | 0.366 | 0.273 | 0.427 | 0.070 | 0.343 |
| init=1.0 | 0.131 | 0.277 | 0.293 | 0.082 | 0.833 | 0.418 | 0.465 | 0.207 | 0.457 | 0.383 | 0.516 | 0.199 | 0.467 | 0.306 | 0.466 | 0.063 | 0.348 |
| init=1.1 | 0.200 | 0.230 | 0.309 | 0.050 | 0.847 | 0.420 | 0.465 | 0.207 | 0.457 | 0.386 | 0.516 | 0.199 | 0.547 | 0.331 | 0.495 | 0.064 | 0.358 |
| init=1.2 | 0.278 | 0.195 | 0.331 | 0.042 | 0.848 | 0.422 | 0.582 | 0.207 | 0.478 | 0.388 | 0.516 | 0.199 | 0.608 | 0.350 | 0.528 | 0.088 | 0.379 |
| init=1.3 | 0.340 | 0.167 | 0.359 | 0.048 | 0.850 | 0.423 | 0.493 | 0.207 | 0.509 | 0.388 | 0.516 | 0.199 | 0.656 | 0.362 | 0.551 | 0.094 | 0.385 |
| init=1.4 | 0.390 | 0.145 | 0.385 | 0.059 | 0.851 | 0.424 | 0.607 | 0.207 | 0.516 | 0.390 | 0.517 | 0.199 | 0.696 | 0.373 | 0.568 | 0.095 | 0.401 |
| init=1.5 | 0.430 | 0.126 | 0.409 | 0.074 | 0.851 | 0.425 | 0.563 | 0.197 | 0.523 | 0.390 | 0.501 | 0.199 | 0.727 | 0.382 | 0.581 | 0.122 | 0.406 |
| init=1.6 | 0.463 | 0.110 | 0.429 | 0.094 | 0.852 | 0.425 | 0.618 | 0.209 | 0.525 | 0.391 | 0.509 | 0.199 | 0.752 | 0.390 | 0.594 | 0.116 | 0.417 |
| init=1.7 | 0.491 | 0.096 | 0.445 | 0.109 | 0.852 | 0.425 | 0.593 | 0.211 | 0.526 | 0.391 | 0.597 | 0.199 | 0.773 | 0.395 | 0.609 | 0.142 | 0.429 |
| init=1.8 | 0.515 | 0.086 | 0.462 | 0.121 | 0.853 | 0.426 | 0.584 | 0.222 | 0.527 | 0.392 | 0.600 | 0.197 | 0.791 | 0.400 | 0.622 | 0.158 | 0.435 |
| init=1.9 | 0.534 | 0.076 | 0.474 | 0.133 | 0.853 | 0.426 | 0.604 | 0.222 | 0.527 | 0.392 | 0.606 | 0.200 | 0.807 | 0.404 | 0.631 | 0.163 | 0.441 |
| init=2.0 | 0.550 | 0.068 | 0.485 | 0.141 | 0.853 | 0.426 | 0.644 | 0.224 | 0.528 | 0.392 | 0.604 | 0.203 | 0.820 | 0.407 | 0.638 | 0.169 | 0.447 |

| NLL | TransE | | | | ComplEx | | | | DistMult | | | | RotatE | | | | Average |
|----------|--------|--------|--------|-----------|---------|--------|-------|-----------|----------|---------|-------|-----------|--------|--------|--------|-----------|---------|
| | WN18 | WN18RR | FB15K | FB15K-237 | WN18 | WN18RR | FB15K | FB15K-237 | WN18 | WN18RR | FB15K | FB15K-237 | WN18 | WN18RR | FB15K | FB15K-237 | |
| init=0 | -1.714 | 1.977 | -0.694 | 0.791 | 2.287 | 3.210 | 1.349 | 2.908 | 2.841 | 3.253 | 1.314 | 3.099 | -3.229 | 1.540 | -0.515 | 1.145 | 1.223 |
| init=0.1 | -1.422 | 2.230 | -0.296 | 0.791 | 2.287 | 3.210 | 1.349 | 2.908 | 2.841 | 3.253 | 1.314 | 3.099 | -2.814 | 1.620 | -0.452 | 1.150 | 1.317 |
| init=0.2 | -0.209 | 3.154 | 0.492 | 1.014 | 2.287 | 3.211 | 1.356 | 2.909 | 2.843 | 3.253 | 1.318 | 3.104 | -1.858 | 1.738 | -0.316 | 1.166 | 1.591 |
| init=0.3 | 0.378 | 3.833 | 0.493 | 1.014 | 2.288 | 3.211 | 1.356 | 2.910 | 2.843 | 3.253 | 1.319 | 3.104 | -1.191 | 2.238 | -0.315 | 1.165 | 1.744 |
| init=0.4 | 0.786 | 4.312 | 0.498 | 1.012 | 2.288 | 3.211 | 1.356 | 2.910 | 2.843 | 3.253 | 1.319 | 3.104 | -0.549 | 2.683 | 1.189 | 1.166 | 1.961 |
| init=0.5 | 1.172 | 4.722 | 1.926 | 1.016 | 2.288 | 4.151 | 1.356 | 2.910 | 2.843 | 4.318 | 1.319 | 3.105 | -0.187 | 3.085 | 1.339 | 1.166 | 2.283 |
| init=0.6 | 1.494 | 5.037 | 2.077 | 2.197 | 2.288 | 4.852 | 1.356 | 2.910 | 2.843 | 5.461 | 1.319 | 3.105 | 0.125 | 3.460 | 1.501 | 1.166 | 2.574 |
| init=0.7 | 1.777 | 5.317 | 2.191 | 2.374 | 2.288 | 5.459 | 1.356 | 2.910 | 2.843 | 5.889 | 1.319 | 3.105 | 0.395 | 3.839 | 1.682 | 1.167 | 2.744 |
| init=0.8 | 2.037 | 5.560 | 2.322 | 2.542 | 3.267 | 6.058 | 1.356 | 2.910 | 2.843 | 6.328 | 1.319 | 3.105 | 0.637 | 4.125 | 1.825 | 2.429 | 3.042 |
| init=0.9 | 2.261 | 5.773 | 2.434 | 2.710 | 3.937 | 6.483 | 1.357 | 2.910 | 2.843 | 6.642 | 1.319 | 3.106 | 0.847 | 4.456 | 1.902 | 2.582 | 3.223 |
| init=1.0 | 2.462 | 5.965 | 2.536 | 2.889 | 4.350 | 6.965 | 1.357 | 2.911 | 2.843 | 7.119 | 1.319 | 3.106 | 1.036 | 4.698 | 2.033 | 2.743 | 3.396 |
| init=1.1 | 2.651 | 6.142 | 2.635 | 3.006 | 5.567 | 7.214 | 1.357 | 2.911 | 2.844 | 7.429 | 1.319 | 3.106 | 1.219 | 4.929 | 2.149 | 2.727 | 3.575 |
| init=1.2 | 2.820 | 6.302 | 2.743 | 3.155 | 5.739 | 7.427 | 2.960 | 2.911 | 3.803 | 7.687 | 1.319 | 3.106 | 1.383 | 5.144 | 2.293 | 3.136 | 3.871 |
| init=1.3 | 2.975 | 6.453 | 2.844 | 3.328 | 6.148 | 7.606 | 2.410 | 2.911 | 4.791 | 7.751 | 1.319 | 3.106 | 1.538 | 5.312 | 2.407 | 3.201 | 4.006 |
| init=1.4 | 3.121 | 6.597 | 2.934 | 3.421 | 6.262 | 7.852 | 3.194 | 2.911 | 5.248 | 8.071</ | | | | | | | |

Table 14: Effect of different learning rate in KGEC on the performance of various KGE models across multiple datasets. For all the three metrics, the lower the better.

| ECE | TransE | | | | ComplEx | | | | DistMult | | | | RotatE | | | | Average |
|----------|--------|--------|-------|-----------|---------|--------|-------|-----------|----------|--------|-------|-----------|--------|--------|-------|-----------|---------|
| | WN18 | WN18RR | FB15K | FB15K-237 | WN18 | WN18RR | FB15K | FB15K-237 | WN18 | WN18RR | FB15K | FB15K-237 | WN18 | WN18RR | FB15K | FB15K-237 | |
| lr=0.001 | 0.184 | 0.229 | 0.469 | 0.098 | 0.852 | 0.423 | 0.644 | 0.228 | 0.528 | 0.389 | 0.659 | 0.220 | 0.492 | 0.381 | 0.498 | 0.191 | 0.405 |
| lr=0.002 | 0.172 | 0.231 | 0.517 | 0.052 | 0.852 | 0.423 | 0.608 | 0.227 | 0.527 | 0.388 | 0.596 | 0.218 | 0.476 | 0.371 | 0.456 | 0.092 | 0.388 |
| lr=0.003 | 0.199 | 0.265 | 0.534 | 0.099 | 0.851 | 0.423 | 0.593 | 0.226 | 0.527 | 0.388 | 0.594 | 0.212 | 0.481 | 0.361 | 0.467 | 0.092 | 0.395 |
| lr=0.004 | 0.203 | 0.276 | 0.535 | 0.138 | 0.851 | 0.422 | 0.595 | 0.222 | 0.526 | 0.387 | 0.605 | 0.191 | 0.478 | 0.353 | 0.480 | 0.098 | 0.398 |
| lr=0.005 | 0.179 | 0.281 | 0.521 | 0.157 | 0.850 | 0.422 | 0.594 | 0.213 | 0.525 | 0.386 | 0.612 | 0.178 | 0.479 | 0.344 | 0.476 | 0.092 | 0.394 |
| lr=0.006 | 0.202 | 0.286 | 0.520 | 0.160 | 0.849 | 0.421 | 0.678 | 0.207 | 0.522 | 0.386 | 0.683 | 0.178 | 0.477 | 0.333 | 0.483 | 0.091 | 0.405 |
| lr=0.007 | 0.201 | 0.291 | 0.497 | 0.166 | 0.849 | 0.421 | 0.678 | 0.189 | 0.517 | 0.385 | 0.683 | 0.178 | 0.472 | 0.323 | 0.462 | 0.110 | 0.401 |
| lr=0.008 | 0.188 | 0.287 | 0.491 | 0.163 | 0.846 | 0.419 | 0.678 | 0.189 | 0.495 | 0.384 | 0.683 | 0.178 | 0.466 | 0.317 | 0.455 | 0.127 | 0.398 |
| lr=0.009 | 0.188 | 0.284 | 0.478 | 0.167 | 0.843 | 0.419 | 0.678 | 0.189 | 0.446 | 0.384 | 0.683 | 0.178 | 0.467 | 0.313 | 0.463 | 0.097 | 0.392 |
| lr=0.010 | 0.171 | 0.280 | 0.459 | 0.150 | 0.833 | 0.418 | 0.678 | 0.189 | 0.446 | 0.383 | 0.683 | 0.178 | 0.467 | 0.307 | 0.466 | 0.094 | 0.388 |
| lr=0.020 | 0.152 | 0.246 | 0.380 | 0.064 | 0.699 | 0.392 | 0.678 | 0.189 | 0.446 | 0.353 | 0.683 | 0.178 | 0.514 | 0.273 | 0.560 | 0.239 | 0.378 |
| lr=0.030 | 0.184 | 0.228 | 0.460 | 0.080 | 0.699 | 0.374 | 0.677 | 0.189 | 0.446 | 0.349 | 0.683 | 0.178 | 0.562 | 0.289 | 0.606 | 0.238 | 0.390 |
| lr=0.040 | 0.244 | 0.211 | 0.507 | 0.114 | 0.699 | 0.374 | 0.678 | 0.189 | 0.446 | 0.349 | 0.683 | 0.178 | 0.598 | 0.290 | 0.638 | 0.097 | 0.393 |
| lr=0.050 | 0.305 | 0.189 | 0.530 | 0.139 | 0.699 | 0.374 | 0.677 | 0.189 | 0.446 | 0.349 | 0.682 | 0.178 | 0.623 | 0.295 | 0.652 | 0.238 | 0.410 |
| lr=0.060 | 0.342 | 0.163 | 0.554 | 0.212 | 0.699 | 0.364 | 0.677 | 0.189 | 0.446 | 0.205 | 0.683 | 0.178 | 0.635 | 0.330 | 0.674 | 0.237 | 0.412 |
| lr=0.070 | 0.393 | 0.153 | 0.569 | 0.164 | 0.699 | 0.374 | 0.677 | 0.190 | 0.526 | 0.349 | 0.683 | 0.178 | 0.656 | 0.330 | 0.679 | 0.239 | 0.429 |
| lr=0.080 | 0.418 | 0.135 | 0.577 | 0.174 | 0.699 | 0.407 | 0.678 | 0.189 | 0.446 | 0.349 | 0.682 | 0.178 | 0.685 | 0.332 | 0.680 | 0.239 | 0.429 |
| lr=0.090 | 0.456 | 0.130 | 0.584 | 0.184 | 0.826 | 0.374 | 0.677 | 0.189 | 0.446 | 0.385 | 0.683 | 0.178 | 0.716 | 0.350 | 0.693 | 0.237 | 0.444 |
| lr=0.100 | 0.494 | 0.108 | 0.590 | 0.193 | 0.699 | 0.374 | 0.677 | 0.189 | 0.527 | 0.349 | 0.683 | 0.178 | 0.742 | 0.331 | 0.696 | 0.239 | 0.442 |

| ACE | TransE | | | | ComplEx | | | | DistMult | | | | RotatE | | | | Average |
|----------|--------|--------|-------|-----------|---------|--------|-------|-----------|----------|--------|-------|-----------|--------|--------|-------|-----------|---------|
| | WN18 | WN18RR | FB15K | FB15K-237 | WN18 | WN18RR | FB15K | FB15K-237 | WN18 | WN18RR | FB15K | FB15K-237 | WN18 | WN18RR | FB15K | FB15K-237 | |
| lr=0.001 | 0.220 | 0.237 | 0.276 | 0.098 | 0.852 | 0.423 | 0.644 | 0.227 | 0.527 | 0.388 | 0.659 | 0.219 | 0.492 | 0.380 | 0.498 | 0.190 | 0.396 |
| lr=0.002 | 0.171 | 0.236 | 0.248 | 0.037 | 0.851 | 0.423 | 0.587 | 0.226 | 0.527 | 0.388 | 0.562 | 0.216 | 0.459 | 0.370 | 0.456 | 0.069 | 0.364 |
| lr=0.003 | 0.119 | 0.263 | 0.247 | 0.049 | 0.851 | 0.423 | 0.513 | 0.225 | 0.526 | 0.388 | 0.547 | 0.205 | 0.457 | 0.361 | 0.445 | 0.069 | 0.356 |
| lr=0.004 | 0.108 | 0.273 | 0.252 | 0.075 | 0.851 | 0.422 | 0.486 | 0.220 | 0.525 | 0.387 | 0.499 | 0.198 | 0.457 | 0.352 | 0.437 | 0.063 | 0.350 |
| lr=0.005 | 0.109 | 0.278 | 0.256 | 0.092 | 0.850 | 0.422 | 0.527 | 0.211 | 0.524 | 0.386 | 0.497 | 0.199 | 0.461 | 0.344 | 0.440 | 0.067 | 0.354 |
| lr=0.006 | 0.107 | 0.283 | 0.264 | 0.095 | 0.849 | 0.421 | 0.465 | 0.208 | 0.521 | 0.386 | 0.516 | 0.199 | 0.463 | 0.333 | 0.435 | 0.065 | 0.351 |
| lr=0.007 | 0.112 | 0.288 | 0.264 | 0.101 | 0.849 | 0.421 | 0.465 | 0.207 | 0.514 | 0.385 | 0.516 | 0.199 | 0.465 | 0.323 | 0.448 | 0.066 | 0.351 |
| lr=0.008 | 0.122 | 0.284 | 0.272 | 0.097 | 0.845 | 0.419 | 0.465 | 0.207 | 0.488 | 0.384 | 0.516 | 0.199 | 0.466 | 0.317 | 0.452 | 0.071 | 0.350 |
| lr=0.009 | 0.127 | 0.281 | 0.284 | 0.100 | 0.842 | 0.419 | 0.465 | 0.207 | 0.457 | 0.384 | 0.516 | 0.199 | 0.467 | 0.313 | 0.463 | 0.062 | 0.349 |
| lr=0.010 | 0.131 | 0.277 | 0.293 | 0.082 | 0.833 | 0.418 | 0.465 | 0.207 | 0.457 | 0.383 | 0.516 | 0.199 | 0.467 | 0.306 | 0.466 | 0.063 | 0.348 |
| lr=0.020 | 0.146 | 0.244 | 0.400 | 0.048 | 0.689 | 0.392 | 0.465 | 0.207 | 0.457 | 0.352 | 0.517 | 0.199 | 0.514 | 0.273 | 0.560 | 0.994 | 0.404 |
| lr=0.030 | 0.163 | 0.227 | 0.471 | 0.075 | 0.689 | 0.160 | 0.484 | 0.207 | 0.457 | 0.238 | 0.517 | 0.199 | 0.562 | 0.289 | 0.606 | 1.010 | 0.397 |
| lr=0.040 | 0.244 | 0.211 | 0.511 | 0.114 | 0.689 | 0.160 | 0.466 | 0.207 | 0.457 | 0.238 | 0.522 | 0.199 | 0.598 | 0.290 | 0.638 | 0.085 | 0.352 |
| lr=0.050 | 0.305 | 0.191 | 0.535 | 0.139 | 0.689 | 0.160 | 0.486 | 0.207 | 0.457 | 0.238 | 0.529 | 0.199 | 0.623 | 0.295 | 0.652 | 1.115 | 0.426 |
| lr=0.060 | 0.342 | 0.167 | 0.554 | 2.220 | 0.689 | 0.364 | 0.493 | 0.207 | 0.457 | 0.189 | 0.519 | 0.199 | 0.635 | 0.330 | 0.674 | 1.067 | 0.569 |
| lr=0.070 | 0.393 | 0.157 | 0.569 | 0.164 | 0.689 | 0.160 | 0.493 | 0.212 | 0.526 | 0.238 | 0.518 | 0.199 | 0.656 | 0.330 | 0.679 | 0.987 | 0.436 |
| lr=0.080 | 0.418 | 0.139 | 0.577 | 0.174 | 0.689 | 0.407 | 0.469 | 0.207 | 0.457 | 0.238 | 0.533 | 0.199 | 0.685 | 0.332 | 0.680 | 0.986 | 0.449 |
| lr=0.090 | 0.456 | 0.136 | 0.584 | 0.184 | 0.826 | 0.160 | 0.503 | 0.208 | 0.457 | 0.383 | 0.517 | 0.200 | 0.716 | 0.350 | 0.693 | 1.142 | 0.470 |
| lr=0.100 | 0.494 | 0.114 | 0.590 | 0.193 | 0.689 | 0.160 | 0.498 | 0.208 | 0.527 | 0.240 | 0.521 | 0.200 | 0.742 | 0.331 | 0.696 | 0.997 | 0.450 |

| NLL | TransE | | | | ComplEx | | | | DistMult | | | | RotatE | | | | Average |
|----------|--------|--------|-------|-----------|---------|--------|-------|-----------|----------|--------|-------|-----------|--------|--------|-------|-----------|---------|
| | WN18 | WN18RR | FB15K | FB15K-237 | WN18 | WN18RR | FB15K | FB15K-237 | WN18 | WN18RR | FB15K | FB15K-237 | WN18 | WN18RR | FB15K | FB15K-237 | |
| lr=0.001 | 2.751 | 6.481 | 2.469 | 3.771 | 6.777 | 7.749 | 3.691 | 7.271 | 7.279 | 7.797 | 4.071 | 7.207 | 1.254 | 5.847 | 2.159 | 4.410 | 5.061 |
| lr=0.002 | 2.505 | 6.267 | 2.341 | 3.233 | 6.634 | 7.665 | 3.006 | 6.945 | 7.073 | 7.729 | 2.871 | 6.351 | 1.014 | 5.546 | 1.997 | 2.862 | 4.627 |
| lr=0.003 | 2.471 | 6.029 | 2.309 | 3.034 | 6.514 | 7.599 | 2.511 | 6.618 | 6.818 | 7.646 | 2.763 | 5.263 | 1.008 | 5.357 | 1.961 | 2.860 | 4.423 |
| lr=0.004 | 2.468 | 5.984 | 2.311 | 2.924 | 6.292 | 7.493 | 2.301 | 5.853 | 6.526 | 7.562 | 2.353 | 3.975 | 1.010 | 5.217 | 1.934 | 2.703 | 4.182 |
| lr=0.005 | 2.473 | 5.966 | 2.331 | 2.865 | 6.188 | 7.455 | 2.587 | 4.799 | 6.230 | 7.495 | 2.256 | 3.106 | 1.019 | 5.101 | 1.942 | 2.817 | 4.039 |
| lr=0.006 | 2.464 | 5.947 | 2.353 | 2.853 | 5.874 | 7.356 | 1.357 | 4.372 | 5.670 | 7.383 | 1.319 | 3.106 | 1.024 | 4.965 | 1.927 | 2.793 | 3.798 |
| lr=0.007 | 2.462 | 5.931 | 2.406 | 2.834 | 5.773 | 7.280 | 1.357 | 2.911 | 5.093 | 7.362 | 1.319 | 3.106 | 1.028 | 4.857 | 1.970 | 2.635 | 3.645 |
| lr=0.008 | 2.466 | 5.942 | 2.444 | 2.845 | 5.288 | 7.094 | 1.357 | 2.911 | 4.088 | 7.253 | 1.319 | 3.106 | 1.032 | 4.800 | 1.984 | 2.573 | 3.531 |
| lr=0.009 | 2.465 | 5.951 | 2.473 | 2.831 | 4.963 | 7.113 | 1.357 | 2.911 | 2.843 | 7.203 | 1.319 | 3.106 | 1.033 | 4.757 | 2.026 | 2.711 | 3.441 |
| lr=0.010 | 2.462 | 5.965 | 2.536 | 2.889 | 4.350 | 6.965 | 1.357 | 2.911 | 2.843 | 7.119 | 1.319 | 3.106 | 1.036 | 4.698 | 2.033 | 2.743 | 3.396 |
| lr=0.020 | 2.519 | 6.087 | 3.006 | 3.237 | 2.288 | 5.673 | 1.356 | 2.911 | 2.844 | 5.811 | 1.319 | 3.106 | 1.146 | 4.446 | 2.456 | 1.167 | 3.086 |
| lr=0.030 | 2.579 | 6.160 | 3.362 | 3.546 | 2.288 | 3.211 | 1.351 | 2.910 | 2.844 | 3.254 | 1.320 | 3.106 | 1.274 | 4.564 | 2.756 | 1.167 | 2.856 |
| lr=0.040 | 2.747 | 6.236 | 3.661 | 3.855 | 2.288 | 3.211 | 1.356 | 2.910 | 2.844 | 3.254 | 1.320 | 3.106 | 1.370 | 4.575 | 3.027 | 3.067 | 3.052 |
| lr=0.050 | 2.896 | 6.335 | 3.839 | 4.096 | 2.288 | 3.211 | 1.352 | 2.910 | 2.844 | 3.254 | 1.315 | 3.106 | 1.436 | 4.608 | 3.173 | 1.159 | 2.989 |
| lr=0.060 | 2.990 | 6.475 | 4.068 | 0.967 | 2.288 | 5.092 | 1.350 | 2.910 | 2.844 | 4.147 | 1.322 | 3.106 | 1.474 | 4.934 | 3.466 | 1.167 | 3.037 |
| lr=0.070 | 3.149 | 6.532 | 4.254 | 4.399 | 2.288 | 3.211 | 1.350 | 2.909 | 6.683 | 3.253 | 1.321 | 3.106 | 1.531 | 4.920 | 3.546 | 1.177 | 3.352 |
| lr=0.080 | 3.225 | 6.648 | 4.370 | 4.564 | 2.288 | 6.227 | 1.361 | 2.910 | 2.844 | 3.253 | 1.315 | 3.105 | 1.640 | 4.945 | 3.557 | 1.177 | 3.339 |
| lr=0.090 | 3.366 | 6.692 | 4.495 | 4.759 | 4.059 | 3.211 | 1.350 | 2.910 | 2.844 | 7.289 | 1.319 | 3.105 | 1.767 | 5.153 | 3.803 | 1.171 | 3.581 |
| lr=0.100 | 3.533 | 6.874 | 4.587 | 4.993 | 2.288 | 3.211 | 1.350 | 2.910 | 7.271 | 3.253 | 1.321 | 3.105 | 1.887 | 4.928 | 3.867 | 1.174 | 3.534 |